Highly Functionalized Dimeric Tetraethynylethenes and Expanded Radialenes: Strong Evidence for Macrocyclic Cross-Conjugation

Mogens Brøndsted Nielsen,[a] Martin Schreiber,[a] Yong Gu Baek,[a] Paul Seiler,[a] Steve Lecomte,[b] Corinne Boudon,[c] Rik R. Tykwinski,[d] Jean-Paul Gisselbrecht,[c] Volker Gramlich,[e] Philip J. Skinner,[a] Christian Bosshard,[b] Peter Günter,[b] Maurice Gross,[c] and François Diederich*[a]

Dedicated to Professor Heinz A. Staab on the occasion of his 75th birthday

Abstract: A selection of dimeric tetraethynylethenes (TEEs) and perethynylated expanded radialenes, containing different donor/acceptor substitution patterns, have been prepared and fully characterized. The first X-ray crystal structure of an expanded [6]radialene, with twelve peripheral 3,5-di(*tert*-butyl)-phenyl substituents, is presented. This macrocycle, the all-carbon core of which is isomeric with fullerene C_{60}, adopts a non-planar, "chair-like" conformation. Also a TEE dimer, carrying *N*,*N*-dimethylaniline donor substituents, has been subjected to an X-ray crystallographic analysis. The electronic properties were studied by UV/Vis spectroscopy and electrochemistry, providing fundamental insight into mechanisms of π-electron delocalization in the acyclic and macrocyclic chromophores. Donor or donor–acceptor-substituted dimeric TEE derivatives show very strong absorptions extending over the entire UV/Vis region; their longest wavelength absorption bands have high charge-transfer character. Macrocyclic cross-conjugation in the expanded radialenes becomes increasingly efficient with increasing donor–acceptor polarization. A dual, strongly solvent-polarity-dependent fluorescence was observed for a tetrakis(*N*,*N*-dimethylaniline)-substituted dimeric TEE; this interesting emission behavior is explained by the twisted intramolecular charge-transfer (TICT) state model. Donor-substituted expanded radialenes display huge resonance-enhanced third-order nonlinear optical coefficients.

Keywords: alkynes · conjugation · electrochemistry · expanded radialenes · nonlinear optics

[a] Prof. Dr. F. Diederich, Dr. M. B. Nielsen, Dr. M. Schreiber, Dr. Y. G. Baek, P. Seiler, Dr. P. J. Skinner
Laboratorium für Organische Chemie, ETH-Zentrum
Universitätstrasse 16, 8092 Zürich (Switzerland)
Fax: (+41) 1 632 1109
E-mail: diederich@org.chem.ethz.ch

[b] Dipl.-Phys. S. Lecomte, PD Dr. C. Bosshard, Prof. Dr. P. Günter
Nonlinear Optics Laboratory
Institute of Quantum Electronics
ETH-Hönggerberg
8093 Zürich (Switzerland)

[c] Dr. C. Boudon, Dr. J.-P. Gisselbrecht, Prof. M. Gross
Laboratoire d'Electrochimie
et de Chimie Physique du Corps Solide
UMR 7512, C.N.R.S, Université Louis Pasteur
4, rue Blaise Pascal
67000 Strasbourg (France)

[d] Prof. Dr. R. R. Tykwinski
Department of Chemistry
University of Alberta
Edmonton, AB T6G 2G2 (Canada)

[e] Prof. Dr. V. Gramlich
Laboratorium für Kristallographie, ETH-Zentrum
Sonneggstrasse 5, 8092 Zürich (Switzerland)

Introduction

Radialenes are a series of all-methylidene-substituted cycloalkanes of molecular formula C_nH_n (Figure 1) and have attracted much attention for their unusual structural, electronic, and materials properties.[1, 2] Much effort has been devoted to the addition of substituents around the periphery, such as halogen,[3] cyano, and ester residues,[4] and different aromatic and heteroaromatic functionalities.[5]

Upon formal insertion of ethynediyl or buta-1,3-diynediyl moieties into the cyclic radialene framework, the carbon-rich homologous series of expanded radialenes with the molecular formulae $C_{2n}H_n$ and $C_{3n}H_n$, respectively, are obtained.[6] Such macrocycles belong to the growing class of perethynylated cyclic π systems which have attracted high interest as scaffolds for two and three-dimensional carbon networks.[7]

In earlier work,[6] we have employed suitably functionalized derivatives of tetraethynylethene (TEE, 3,4-diethynylhex-3-ene-1,5-diyne) as precursors for macrocyclic oligodiacetylenes.[8] Studies have shown that TEE derivatives are attractive candidates for nonlinear optical (NLO) materials on

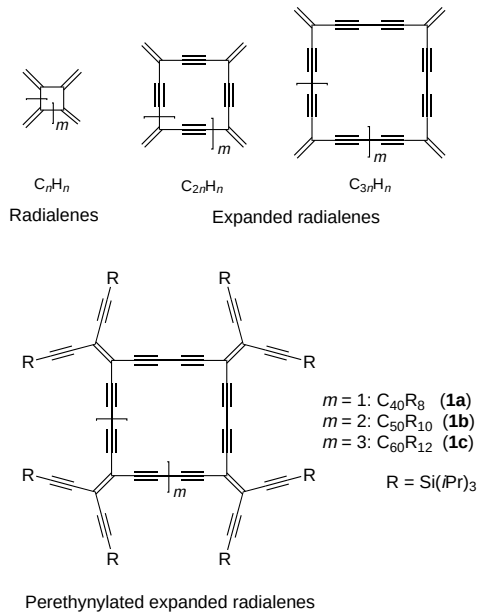

Figure 1. Progression from radialenes to expanded radialenes. As building blocks for the construction of expanded radialenes with peripheral functional groups, tetraethynylethene (TEE) derivatives can be employed.

account of their intrinsic two-dimensional π-electron conjugation pathways.[9] Indeed, donor–acceptor-substituted TEEs display some of the highest known third-order nonlinearities, and, in the case of acentricity, also very large second-order NLO effects. The development of a number of synthetic strategies for preparing differentially silyl-protected TEEs[10] provided suitable modules for the construction of the first series of perethynylated expanded radialenes, **1a–c** (Figure 1).[6] Interestingly, the all-carbon cores of these novel macrocycles can be viewed as isomers of C_{40} (expanded [4]radialene **1a**), C_{50} (expanded [5]radialene **1b**), and C_{60} (expanded [6]radialene **1c**). Electrochemical studies revealed strong electron-acceptor properties of these compounds and a capacity to undergo multiple reduction steps under cyclic voltammetric conditions.[6b] By introducing π-electron donor groups into the periphery, we therefore hoped to further enhance the chromophoric and other physical properties of the perethynylated expanded radialenes. We were also interested to explore, whether π-electron delocalization effects due to macrocyclic cross-conjugation would possibly manifest themselves more strongly in derivatives with donor–acceptor polarization.

Here, we describe the application of acetylenic coupling reactions[11] to the synthesis of three new series of perethynylated expanded radialenes featuring peripheral aryl donor substituents.[12] We include in this investigation the study of donor/acceptor-functionalized TEE dimers which serve as model compounds to evaluate macrocyclic cross-conjugation effects in the expanded radialenes. The physical properties of these two intriguing classes of compounds are investigated by ^{1}H and ^{13}C NMR spectroscopy, electronic absorption, and emission spectroscopy, and electrochemistry. We also report the first X-ray structural characterization of an expanded radialene as well as the redox properties and third-order nonlinear optical properties of these unusual macrocycles.

Results and Discussion

Synthesis: A selection of donor/acceptor-substituted TEEs (such as **2–4**) had been previously synthesized by Sonogashira cross-coupling[13] of vinylic dibromides (**5a**,**b**) with terminal acetylenes.[10b] Selective removal of trimethylsilyl in the presence of triisopropylsilyl protecting groups, followed by oxidative coupling under Hay conditions,[14] had provided TEE dimers, such as **6–8**.[10b] The hexakis[triisopropylsilyl] derivative **9** had also been previously prepared and characterized by X-ray crystallography.[15]

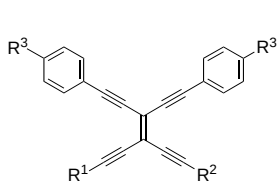

	R^1	R^2	R^3
2a	Si(*i*Pr)$_3$	Si(*i*Pr)$_3$	NMe_2
2b	$SiMe_3$	Si(*i*Pr)$_3$	NMe_2
3a	Si(*i*Pr)$_3$	Si(*i*Pr)$_3$	$N(C_{12}H_{25})_2$
3b	$SiMe_3$	Si(*i*Pr)$_3$	$N(C_{12}H_{25})_2$
4a	Si(*i*Pr)$_3$	Si(*i*Pr)$_3$	NO_2
4b	$SiMe_3$	Si(*i*Pr)$_3$	NO_2

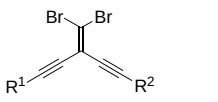

	R^1	R^2
5a	Si(*i*Pr)$_3$	Si(*i*Pr)$_3$
5b	$SiMe_3$	Si(*i*Pr)$_3$
5c	$SiMe_3$	$SiMe_3$

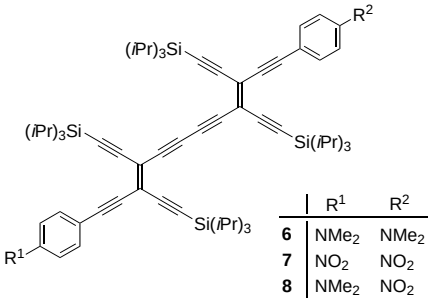

	R^1	R^2
6	NMe_2	NMe_2
7	NO_2	NO_2
8	NMe_2	NO_2

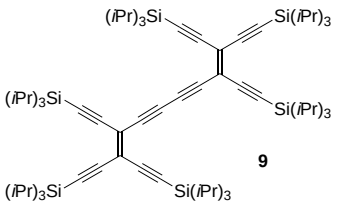

9

The 3,5-di(*tert*-butyl)phenyl-substituted TEEs **10a**,**b** were prepared (Scheme 1) by Sonogashira cross-coupling of dibromides **5b**, **c** with an excess of terminal alkyne **11**.[16] The syntheses of the two TEE derivatives could be substantially optimized relative to a procedure published earlier,[17] which only provided low yields of about 30%. The unsymmetrically protected TEE **10a** was subsequently treated with K_2CO_3 in MeOH/THF, thereby removing selectively the $SiMe_3$ group, and the resulting terminal alkyne was subjected to the Hay coupling conditions (CuCl, *N*,*N*,*N*′,*N*′-tetramethylethylenediamine (TMEDA), CH_2Cl_2) to afford dimeric **12**. Employing the same strategy, dimers **13–15** were prepared in high yields (Scheme 2).

Next, a Hay cross-coupling reaction was carried out by mixing equal amounts of the two TEEs **2b** and **4b** (Scheme 3).

0947-6539/01/0715-3264 $ 17.50+.50/0 *Chem. Eur. J.* **2001**, *7*, No. 15

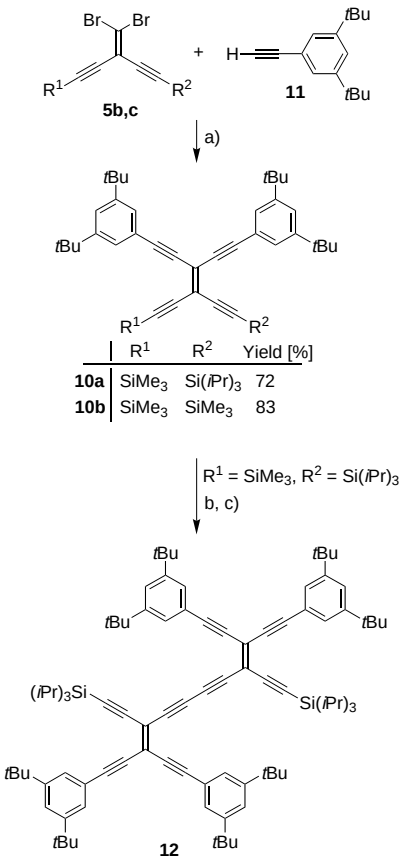

Scheme 1. Synthesis of 3,5-di(*tert*-butyl)phenyl-substituted monomeric and dimeric TEE derivatives **10a**,**b** and **12**. a) CuI, $[PdCl_2(PPh_3)_2]$, THF, $(iPr)_2NH$ or NEt_3. b) K_2CO_3, MeOH/THF. c) CuCl, TMEDA, O_2, CH_2Cl_2, 61 % (steps b and c).

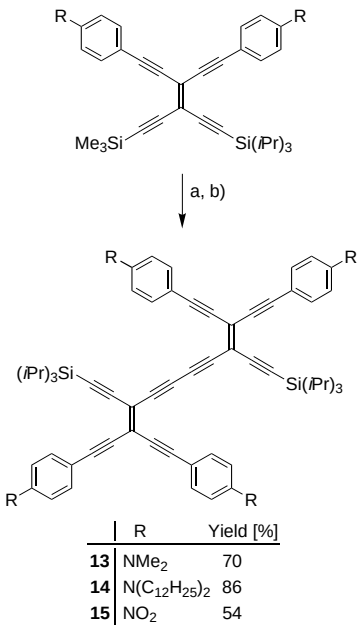

Scheme 2. Synthesis of the donor/acceptor-substituted dimeric TEE derivatives **13**–**15**. a) K_2CO_3, MeOH/THF. b) CuCl, TMEDA, O_2, CH_2Cl_2.

Thus, removal of the $SiMe_3$ groups in the two starting materials, followed by oxidative coupling gave the donor–acceptor dimer **16** together with the homocoupled products **13** and **15** in an approximate 2:1:1 ratio. Two fractions were isolated from column chromatography, the first containing a mixture of **13** and **16** and the second containing pure **15**. Separation of **13** and **16** was accomplished by preparative thin-layer chromatography providing the donor–acceptor derivative in 36 % yield.

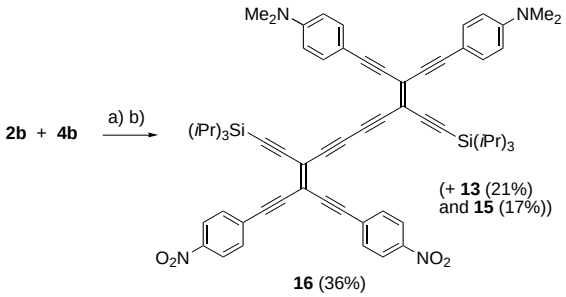

Scheme 3. Synthesis of donor–acceptor-substituted dimeric TEE **16**. a) K_2CO_3, MeOH/THF. b) CuCl, TMEDA, O_2, CH_2Cl_2.

Removal of the $Si(iPr)_3$ groups in dimer **14** with Bu_4NF and subsequent Hay coupling with *p*-nitrophenylacetylene gave dimer **17** featuring an extended, strongly violet-colored donor–acceptor chromophore (Scheme 4). The all-donor-substituted analogue **18** was prepared in a similar way. Large excesses of the phenylacetylenes were employed in these cross-coupling reactions in order to avoid homocoupling of deprotected **14**.

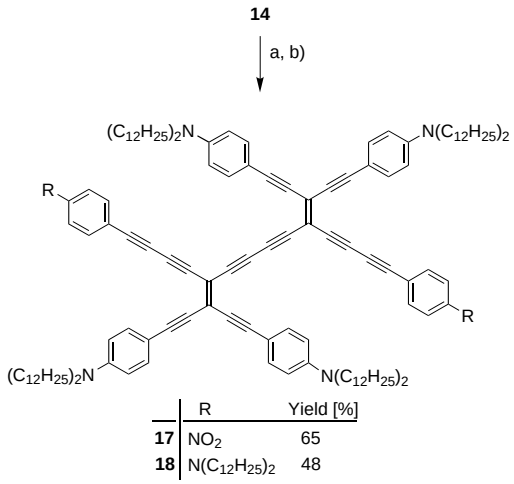

Scheme 4. Synthesis of dimeric TEE derivatives **17** and **18** featuring extended, perarylated chromophores. a) Bu_4NF, THF/H_2O. b) R-*p*-$C_6H_4C{\equiv}CH$ (12 equiv; $R = NO_2$, $N(C_{12}H_{25})_2$), CuCl, TMEDA, O_2, CH_2Cl_2.

In an attempt to introduce liquid crystallinity, we decided to prepare TEEs containing mesogenic (4′-cyanobiphenyl-4-yloxy)undecyl groups.[18] For this purpose, alcohol **19**[19] was converted with CBr_4 and PPh_3 into bromide **20** which reacted with *p*-iodophenol in the presence of NaH to give **21** (Scheme 5). Sonogashira cross-coupling with triisopropylsilylacetylene led to **22** which was silyl-deprotected with Bu_4NF to provide terminal alkyne **23**. Subsequent cross-

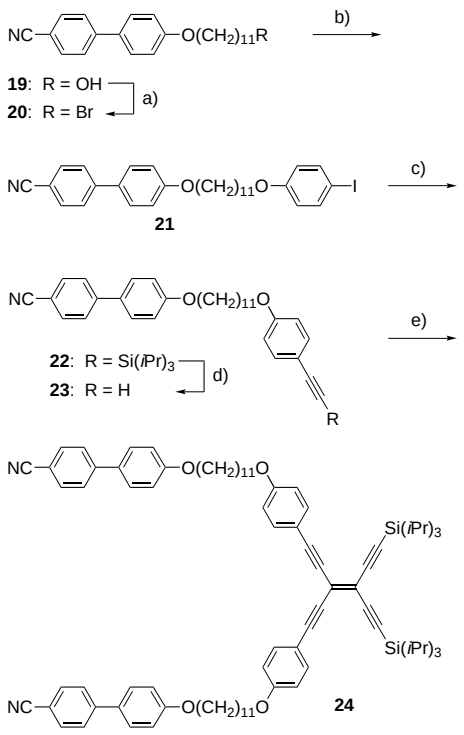

Scheme 5. Synthesis of TEE **24** with appended mesogenic 11-(4′-cyanobiphenyl-4-yloxy)undecyl groups. a) CBr_4, PPh_3, CH_2Cl_2, 92%. b) NaH, *p*-iodophenol, DMF, 79%. c) CuI, $[PdCl_2(PPh_3)_2]$, $iPr_3Si\text{-}C{\equiv}CH$, Bu_4NBr, THF, iPr_2NH, 96%. d) Bu_4NF, THF, 93%. e) CuI, $[PdCl_2(PPh_3)_2]$, **5a**, Bu_4NBr, THF, iPr_2NH, 84%.

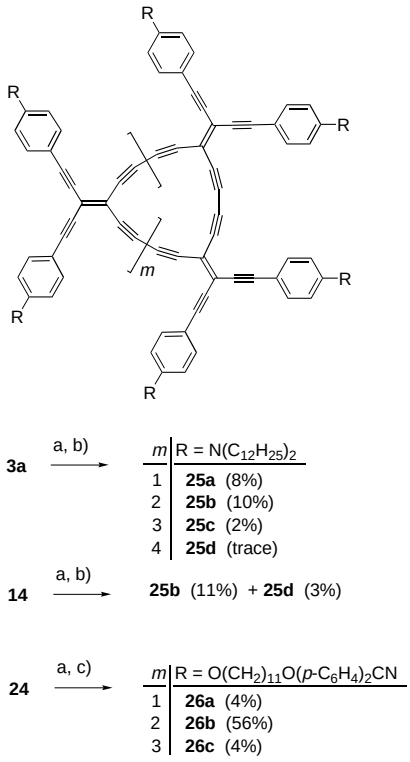

Scheme 6. Synthesis of donor-substituted expanded radialenes **25a–d** and **26a–c**. a) Bu_4NF, THF. b) CuCl, TMEDA, O_2, CH_2Cl_2. c) $Cu(OAc)_2$, O_2, pyridine/benzene.

coupling with vinyl dibromide **5a** afforded TEE **24** in good yield.

In the following, several series of substituted expanded [*n*]radialenes were prepared. Representatives of the donor-functionalized derivatives **25a–d** were obtained by two routes (Scheme 6). In one approach, the two $Si(iPr)_3$ protecting groups of TEE **3a** were removed with Bu_4NF and subsequent Hay coupling under dilute conditions provided the strongly violet-colored macrocycles **25a–d**, which were separated by column chromatography. The expanded [4]radialene **25b** was isolated in highest yield (10%) whereas the largest, hexameric cyclic oligomer **25d** was only formed in trace amounts. The latter could be obtained in somewhat higher yield by silyl-deprotection of the acyclic dimer **14** followed by Hay coupling. Under these conditions, expanded [4]radialene **25b** was formed in 11% and the higher [6]-homologue **25d** in 3% yield. In analogy, oxidative macrocyclization of silyl-deprotected **24** under Eglinton conditions ($Cu(OAc)_2$, pyridine/benzene)[20] provided **26a–c** with laterally appended mesogenic groups.

It was hoped that the expanded radialenes **26a–c** would display good liquid crystalline properties on account of the laterally attached mesogenic groups. However, studies on the major product, cyclic tetramer **26b**, did not reveal such properties. Differential scanning calorimetry showed a sharp but very weak peak. Optical polarized microscopy studies were unsatisfactory as well. One explanation for this negative result may be that domain effects from the radialene were not able to transfer because the alkyl spacers are too long. Therefore, we prepared related expanded radialenes with hexyloxy spacers instead of the undecyloxy spacers. Since this modification did actually not lead to improved properties, the synthesis and characterization of these modified radialenes will not be described here. The expanded [5]radialene with the laterally appended (4′-cyanobiphenyl-4-yloxy)hexyl groups was an amorphous solid, with a glass transition temperature (T_g) of 53 °C. It seems that in order to achieve liquid crystalline phase behavior, further structural modifications will be necessary, which we have not pursued further in the present work. In the context of this study, we were mainly interested in the electronic effects, caused by the attachment of 4-alkoxyphenyl donor substituents in the periphery of the electron-accepting all-carbon core in **26a–c**.

Silyl deprotection of TEE **10b** followed by oxidative cyclization afforded a red-orange mixture of 3,5-di(*tert*-butyl)phenyl-substituted expanded radialenes that was inseparable due to the very small polarity difference between individual compounds (Scheme 7). According to matrix-assisted laser-desorption-ionization mass spectrometry (MALDI-TOF MS) in the negative ion mode with α-cyanocinnamic acid (CCA) as matrix, this mixture contained the [*n*]radialenes **27a–f** with *n* ranging from 3 to 8 as the major products in addition to minor quantities of very large derivatives with $n = 9$, 10. The base peak in the spectrum corresponded to the molecular ion of [6]radialene **27d**, whereas the relative intensities of the peaks assigned to the very large macrocyclic perimeters ($n = 8–10$) were less than 2%. We had previously already observed the formation of such exceptionally large expanded radialenes with terminal

  0947-6539/01/0715-3266 $ 17.50+.50/0 *Chem. Eur. J.* **2001**, *7*, No. 15

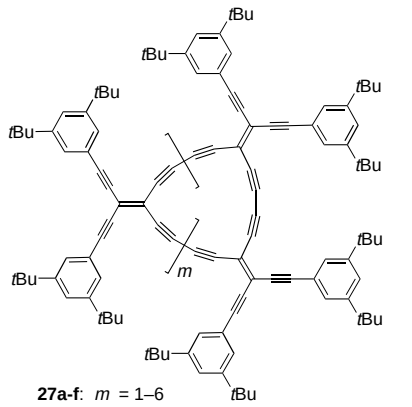

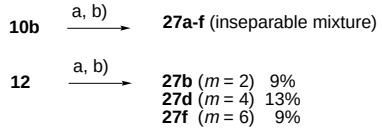

Scheme 7. Synthesis of 3,5-di(*tert*-butyl)phenyl-substituted expanded radialenes **27b**, **d**, **f**. a) Bu_4NF, THF; b) CuCl, TMEDA, O_2, CH_2Cl_2.

$Si(iPr)_3$ groups and even isolated very small quantities as stable materials.[6b] In future work, we intend to prepare larger quantities for full characterization of these compounds possessing all-carbon cores exceeding 100 C atoms.

Gratifyingly, starting from TEE dimer **12**, silyl deprotection and oxidative cyclization provided a crude mixture of the expanded [4]-, [6]-, and [8]radialenes **27b**, **27d**, and **27f** which could be separated by column chromatography (silica gel; eluent hexane/CH_2Cl_2 3:1) followed by gravity gel permeation chromatography (GPC, Bio-Beads S-X1; eluent CH_2Cl_2) (Scheme 7). Analytical GPC (TosoHaas TSKgel G2500HHR column; eluent THF) revealed retention times of 16.3 min (**27b**), 15.8 min (**27d**), and 15.4 min (**27f**) which, according to a polystyrene calibration curve,[21] correspond to compounds with masses of around 2300, 3100, and 3900 Da, respectively, in relatively good agreement with the calculated molecular weights (1995.0, 2992.5, and 3990.0 $g\,mol^{-1}$). The expanded [8]radialene, with a C_{80} core, is the largest member of this new class of macrocyclic chromophores prepared so far.

All TEE dimers are stable compounds. Derivatives **13**, **15**, and **16** all form solids at room temperature. Substituting the methyl groups with dodecyl groups, such as in compound **14**, results in the formation of an oil. The extended dimer **18** forms an oily solid, whereas the related dimer **17** is solid.

The members of the three series of arylated expanded radialenes all showed very good solubility in organic solvents such as CH_2Cl_2 and $CHCl_3$. No special precautions with respect to stability were required in storing the samples. The expanded radialenes **27a–f** displayed, however, a slight light sensitivity. In order to avoid light-induced decomposition, their chromatographic workup was carried out in the dark. The di(dodecylamino)phenyl-substituted expanded radialenes **25a–d** were isolated as oils, whereas the mesogen-substituted derivatives **26a–c** were obtained as solids. The di(*tert*-butyl)phenyl-substituted expanded [4]- and [8]radialenes **27b** and **27f** form oily solids, whereas the [6]radialene derivative **27d** is a solid.

As was noted previously,[6a] MALDI-TOF MS is a powerful tool for the characterization of the expanded radialenes. The spectra of pure compounds mainly displayed the molecular ion as the parent ion with little or no fragmentation being observed, which allowed an unambiguous assignment of the molecular composition. However, for the di(*tert*-butyl)phenyl-substituted expanded radialenes, which contain no heteroatoms, the signal-to-noise ratios were less good.

The ^1H NMR chemical shifts ($CHCl_3$) for the aromatic protons of some selected donor/acceptor-substituted dimeric TEEs and expanded radialenes are given in Table 1. An interesting yet poorly understood effect is revealed by the comparison of the data for the donor–acceptor dimer **16** with

Table 1. Selected ^1H NMR chemical shifts (200 or 500 MHz, $CDCl_3$, 298 K) of aryl protons in mono/dimeric TEEs and expanded radialenes.

Compound	$ArNR_2$ δ				$ArNO_2$ δ			
2a[a]	6.60		7.38					
3a[a]	6.50		7.32					
4a[a]					7.63		8.19	
13	6.51	6.63	7.38	7.41				
14	6.44	6.53	7.33	7.35				
15					7.62	7.69	8.09	8.25
16	6.42	6.64	7.32	7.43	7.54	7.67	7.98	8.24
17	6.47	6.57	7.38	7.44	7.66		8.21	
25a	6.56		7.41					
25b	6.41		7.40					
25c	6.31		7.33					
25d	6.30		7.28					

[a] See ref. [10b].

those for the all-donor- (**13**) and all-acceptor-substituted (**15**) analogues. The aromatic resonances of one 4-$Me_2NC_6H_4$ and one 4-$O_2NC_6H_4$ moiety in **16** are distinctly upfield shifted (by 0.06–0.11 ppm) whereas the corresponding resonances in the second set of these substituents in **16** appears at nearly identical positions ($\Delta\delta = 0.1–0.2$ ppm). Increasing the expanded radialene ring size in the series **25a–d** results in increasing upfield shifts of the aromatic protons. This observation can be explained by the shielding effect of neighboring aryl groups, which approach each other more closely in the higher homologues. Iyoda et al. had previously observed an upfield shift of the phenyl protons in a sterically crowded octaphenyl[4]radialene.[5c] The signals for the two nonequivalent *tert*-butyl groups in **12** ($\delta = 1.29$ and 1.33) were seen to merge into one upfield-shifted signal in the radialenes **27b**, **27d**, and **27f**, positioned at $\delta = 1.17$, 1.23, and 1.23, respectively.

Some selected ^{13}C NMR data for the expanded radialenes **25a–c** and **27b**, **d**, **f** are collected in Table 2.[22] In contrast to what is usually observed for acetylenic macrocycles possessing some degree of ring strain,[23] only small shifts are observed for the ^{13}C(sp) resonances in the expanded radialenes **25a–c** and **27b**, **d**, **f** relative to dimeric TEEs **14** and **12**, which is indicative of low ring strain in the macrocyclic perimeters. Thus, the resonances of the buta-1,3-diynediyl moieties appear at similar positions between $\delta = 82$ and 88 in all

Table 2. Selected ^{13}C NMR (50 or 125 MHz, $CDCl_3$, 298 K) resonances of alkene and alkyne carbon atoms in expanded radialenes and TEE comparison compounds.

Compound	C (alkyne) δ							C (alkene) δ	
3a	86.6	99.6	100.7	105.1				112.2	119.5
12	82.3	83.6	85.9	86.9	101.7	102.0	102.3 102.9	115.1	121.4
14	82.4	84.6	87.0	87.5	100.3	102.7	102.9 103.5	110.5	122.5
25a	84.9	87.4	98.5	103.4				113.4	[a]
25b	83.9	87.5	87.9	104.5				110.2	118.7
25c	83.3	84.5	88.0	104.6				109.5	121.6
27b	84.2	86.4	86.6	103.6				113.9	119.0
27d	83.0	83.2	86.6	104.1				114.1	123.2
27f	82.8	83.3	86.6	104.1				113.9	123.7

[a] Only one resonance observed for the two different alkene C(sp^2) atoms.

derivatives. Remarkably however, one of the exocyclic alkyne resonances ($\delta = 98.5$) in the smaller [3]radialene **25a** is downfield shifted by more than 10 ppm with respect to the corresponding resonance in the larger [4]- and [5]radialenes **25b** and **25c**. Also, one of the exocyclic C(sp^2) atoms shows a significant upfield shift upon decreasing the ring size of the radialene in the **25a–c** series. Thus, the chemical shift value changes from $\delta = 121.6$ (**25c**) to 118.7 (**25b**), and to 113.4 (**25a**). These data could be indicative of an increase in ring strain and/or a particular electronic configuration in the smaller derivative. No significant differences between the IR spectra of **25a–c**, nor between those of **27b**, **d**, **f**, were observed. However, the absence of a $\tilde{\nu}$(≡C-H) stretching band at about 3300 cm^{-1} confirmed that no terminal acetylenes are present, in accordance with the macrocyclic structures.

X-ray crystallography: Single crystals of TEE dimer **13** suitable for X-ray crystallographic analysis were obtained by slow evaporation of a CH_2Cl_2/CH_3CN solution at room temperature. Compound **13** crystallizes in the orthorhombic space group *Pbca* with four molecules in the unit cell. The structure (Figure 2) reveals that the two alkene double bonds in **13** adopt the *s-trans* conformation with respect to the connecting buta-1,3-diynediyl moiety. This conformational preference in the solid state has been exclusively observed for oligo(triacetylene)s containing TEE or (*E*)-1,2-diethynylethene (DEE, (*E*)-hex-3-ene-1,5-diyne) repeat units.[15, 24] Model examinations reveal that the *s-cis* conformation of **13** would be destabilized by steric interactions between neighboring aryl groups of the two TEE moieties. However, this less favorable conformation needs to be adopted by the related dimers **12** and **14** in the macrocyclization reactions affording the expanded radialenes, as described above. Kinetically, this is not problematic since rotations about the C(sp)–C(sp) bonds or C(sp)–C(sp^2) bonds of the central buta-1,3-diynediyl spacer have extremely low activation barriers.[25] The X-ray crystal structure of **13** shows that the two TEE moieties constitute a plane from which the four aryl groups are slightly distorted. Bond lengths and bond angles are in the range expected from previous X-ray crystallographic investigations (Figure 2; see for example refs. [10a, b, 15b, 24]).

We report here the first X-ray crystal structure analysis (Figure 3) of an expanded radialene. Single crystals of **27d** were grown by slow diffusion of hexane into a solution of the

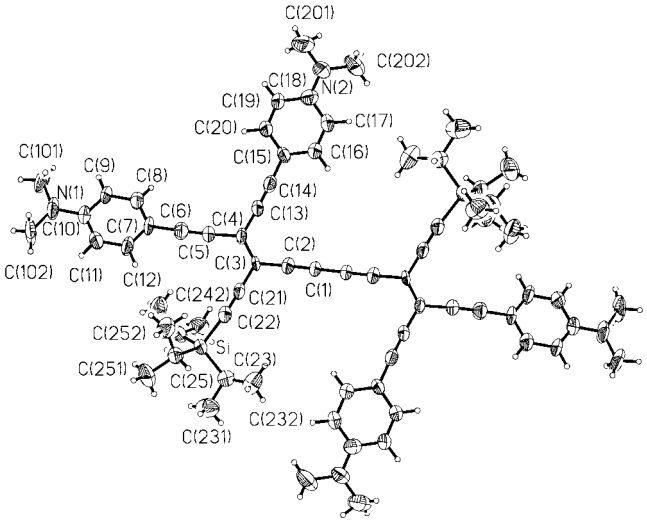

Figure 2. ORTEP plot of **13**; arbitrary numbering,atomic displacement parameters obtained at 293 K are drawn at 50% probability level. Selected bond lengths [Å] and bond angles [°]: C(1)–C(1a) 1.384(9), C(1)–C(2) 1.193(5), C(2)–C(3) 1.419(6), C(3)–C(4) 1.358(5), C(3)–C(21) 1.435(6), C(4)–C(5) 1.432(6), C(4)–C(13) 1.413(6), C(5)–C(6) 1.200(5), C(13)–C(14) 1.206(8), C(21)–C(22) 1.212(5); C(1a)-C(1)-C(2) 178.9(6), C(1)-C(2)-C(3) 177.1(5), C(2)-C(3)-C(4) 121.6(4), C(2)-C(3)-C(21) 116.7(4), C(3)-C(4)-C(5) 120.9(4), C(3)-C(4)-C(13) 122.7(4), C(3)-C(21)-C(22) 177.9(6), C(4)-C(5)-C(6) 176.2(4), C(4)-C(3)-C(21) 121.7(4), C(4)-C(13)-C(14) 175.5(6), C(5)-C(4)-C(13) 116.4(4).

compound in $CDCl_3$. The compound crystallizes in the triclinic space group $P\bar{1}$ with one molecule in the unit cell. The cyclic framework is highly distorted and adopts a chair-like conformation. Three different views of a chair can be considered, either by i) a rectangle defined by C(5)-C(10)-C(5a)-C(10a) and opposite corners C(15a) and C(15) (Figure 3b), ii) a rectangle defined by C(5)-C(15a)-C(5a)-C(15) and opposite corners C(10) and C(10a), or iii) a rectangle defined by C(15)-C(10)-C(15a)-C(10a) and opposite corners C(5) and C(5a). The dimensions of these rectangles are in the range of $10.1 - 11.2 \times 6.6$ Å^2, and the average diagonal distance between C(X) and C(Xa) (X = 5, 10, or 15) is 12.7 Å. The torsional angles in these three chairs are: i) 54.1° [C(15a)-C(5)-C(10)-C(15)], ii) 54.9° [(C(10)-C(5)-C(15a)-C(10a)], and iii) 62.6° [C(5a)-C(15)-C(10)-C(5)], the mean value being 57.2°. For comparison, the torsional angle in the cyclohexane chair is 55.1°.[26]

de Meijere et al.[27a] have carried out X-ray analyses on [*n*]rotanes, perspirocyclopropanated macrocyclic oligodiacetylenes, structurally related to the expanded radialenes, but with insulating C(sp^3) spiro centers separating the buta-1,3-diynediyl fragments instead of alkene C(sp^2) atoms. The [6]rotane **28** of this family of macrocycles also adopts a chair-like conformation in the solid state, but with an average torsional angle of 41.4°, it is less puckered. The difference between these two chair conformations is probably a result of the different steric requirements of the lateral substituents in the two systems, that is steric overcrowding of the bulky 1,5-bis(3,5-di(*tert*-butyl)phenyl)penta-1,4-diyne-3-ylidene residues at the six C(sp^2) "corner atoms" of the macroring enforces a more puckered chair conformation in **27d**.[28] Another example of a chair-formed [6]rotane, persubstituted by ether

0947-6539/01/0715-3268 $ 17.50+.50/0 *Chem. Eur. J.* **2001**, *7*, No. 15

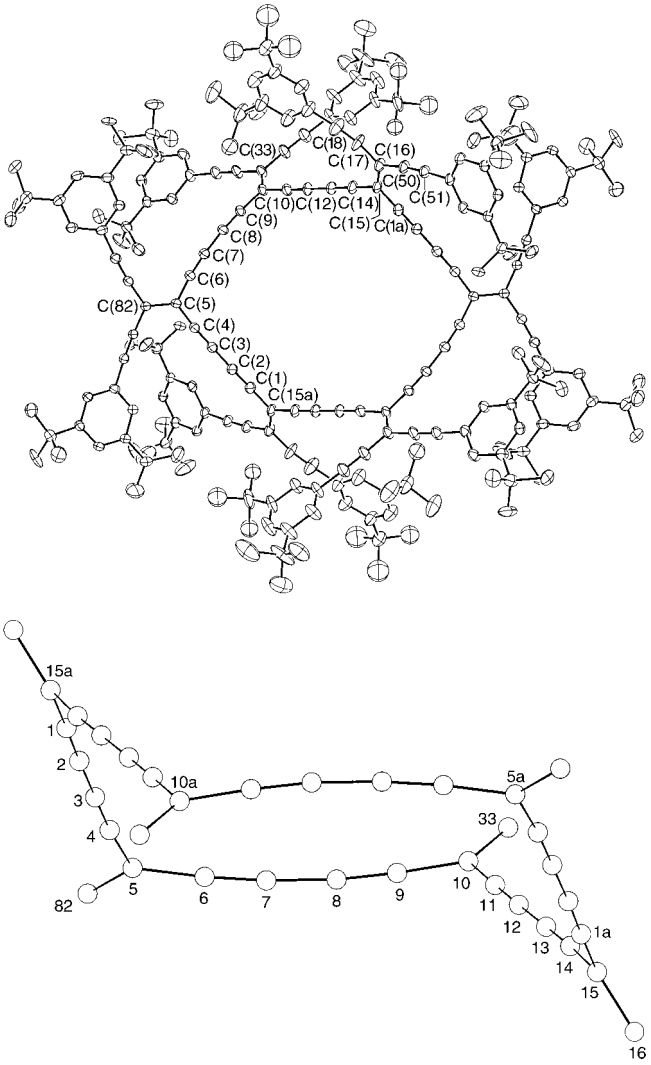

Figure 3. a) ORTEP plot of **27d**; arbitrary numbering, H-atoms are omitted for clarity. Atomic displacement parameters at 203 K are drawn at the 20 % probability level. Selected bond lengths [Å] and bond angles [°]: C(1)–C(15a) 1.415(9), C(1)–C(2) 1.207(8), C(2)–C(3) 1.363(9), C(3)–C(4) 1.208(8), C(4)–C(5) 1.415(8), C(5)–C(6) 1.418(8), C(5)–C(82) 1.386(7), C(6)–C(7) 1.200(8), C(7)–C(8) 1.374(9), C(8)–C(9) 1.192(7), C(9)–C(10) 1.429(8), C(10)–C(33) 1.355(8), C(10)–C(11) 1.435(8), C(11)–C(12) 1.204(8), C(12)–C(13) 1.353(9), C(13)–C(14) 1.190(8), C(14)–C(15) 1.433(8), C(15)–C(16) 1.372(8), C(15)–C(1a) 1.415(9), C(16)–C(17) 1.431(8), C(16)–C(50) 1.389(9), C(17)–C(18) 1.193(7), C(50)–C(51) 1.174(9); C(1)-C(2)-C(3) 178.6(6), C(2)-C(1)-C(15a) 178.9(7), C(2)-C(3)-C(4) 179.1(6), C(3)-C(4)-C(5) 175.2(5), C(4)-C(5)-C(82) 121.9(6), C(4)-C(5)-C(6) 116.0(5), C(5)-C(6)-C(7) 173.4(6), C(6)-C(7)-C(8) 175.1(6), C(6)-C(5)-C(82) 122.2(5), C(7)-C(8)-C(9) 173.7(7), C(8)-C(9)-C(10) 175.7(6), C(9)-C(10)-C(33) 121.5(5), C(9)-C(10)-C(11) 116.8(5), C(10)-C(11)-C(12) 178.8(6), C(11)-C(12)-C(13) 179.3(6), C(11)-C(10)-C(33) 121.7(5), C(12)-C(13)-C(14) 179.9(5), C(13)-C(14)-C(15) 177.3(7), C(14)-C(15)-C(16) 121.4(5), C(14)-C(15)-C(1a) 116.7(5), C(15)-C(16)-C(17) 118.5(5), C(15)-C(16)-C(50) 119.2(5), C(16)-C(17)-C(18) 173.3(6), C(16)-C(15)-C(1a) 121.8(5), C(16)-C(50)-C(51) 170.1(8), C(17)-C(16)-C(50) 122.2(6); b) view on the chair conformation of the macrocyclic core and the exocyclic double bonds in the X-ray crystal structure of **27d**.

functionalities, was provided by Bunz and co-workers.[27b] It is also noteworthy that some [6]radialenes adopt a chair-like conformation as well, as shown by X-ray analysis for hexaethylidenecyclohexane **29**[29a] and dodecamethyl[6]radialene **30**[29b] (see Figure 4). However, in the structure of

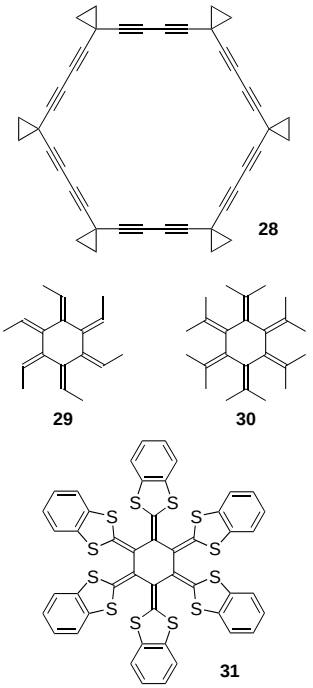

Figure 4. [6]Rotane **28**[27a] and the two [6]radialenes **29**,[29a] and **30**[29b] adopt chair conformations whereas [6]radialene **31**[5d] prefers a boat-shaped geometry in the solid state.

hexakis(4,5-benzo-1,3-dithiol-2-ylidene)cyclohexane (**31**), the conformation is boat-shaped.[5d] Another interesting class of acetylenic macrocycles are the *meta*-cyclo(phenylethynylene)s in which the hexamers have nearly planar rings.[30]

The lengths of the triple bonds within the macrocyclic core of **27d** range from about 1.19 to 1.21 Å, those of the C(sp)–C(sp) single bonds from 1.35 to 1.37 Å, those of the C(sp)–"corner"-C(sp^2) single bonds from 1.42 to 1.43 Å, and those of the exocyclic double bonds from 1.35 to 1.39 Å. Hence, they are almost identical to the corresponding bond lengths in the acyclic TEE dimer **13**. The buta-1,3-diynediyl moieties deviate slightly from linearity, as can be seen from the corresponding bond angles, which vary from ca. 174 to 180°. The [C(sp)-C(sp^2)-C(sp)] bond angles at the "corner atoms" vary from 116 to 117°, whereas the corresponding bond angles at the exocyclic C(sp^2) atoms adopt values between 120 and 122°. The six individual TEE units in **27d** are almost planar. The maximum distortion occurs in the TEE sub-unit [C(1a), C(15), C(14), C(16), C(17), C(50)], with deviations up to 0.03 Å from the mean plane. The *tert*-butyl groups are highly disordered. For seven groups, two orientations were refined by constraining the individual groups to approximately tetrahedral symmetry and bond lengths of about 1.54 Å. In Figure 3, only one orientation is shown for clarity. A disordered hexane with population parameter (pp) of about 0.5 is sitting above and below (due to symmetry) the macrocyclic core (not shown). Moreover, weak electron density peaks were found in three distinct regions of the asymmetric unit, resulting probably from three highly disordered hexane molecules (see Experimental Section). In that respect, it is interesting to compare recent studies of Höger et al.[31] on rigid phenylacetylene-based macrocycles contain-

ing flexible alkyl side chains. One such macrocycle was found to fill its cavity with its own four side chains, with two pointing above and two below the macroring.

Electronic absorption spectroscopy: The UV/Vis spectral data in $CHCl_3$ of the TEE dimers and the expanded radialenes prepared in this study are displayed in Table 3. A joint discussion of the electronic properties of the two classes of compounds is justified by the fact that the dimers contain the 3,4,9,10-tetraalkynyl-substituted dodeca-3,9-diene-1,5,7,11-tetrayne chromophore in a preferred *s-trans* conformation (see Figure 2) which, in the enforced *s-cis* conformation, is also the longest linearly conjugated π-electron fragment in the macrocycles. We hoped that comparisons between the two classes of compounds would reveal particular macrocyclic effects and enable us to recognize whether macrocyclic cross-conjugation in the expanded radialenes would possibly lead to enhanced π-electron delocalization.

As a first important observation, the spectra of the dimeric TEE derivatives (Figure 5, Table 3) confirm in an impressive way the previously recognized[32] strong electron-accepting properties of the central conjugated C_{20} core with its 16 C(sp) atoms. Intramolecular charge-transfer (CT) interactions are nearly equally efficient in the all-donor-substituted dimers such as **13** and **18** than in the donor–acceptor-substituted push–pull systems such as **16** and **17**. The UV/Vis spectra of these compounds display broad absorption shoulders at lower energy with end-absorptions extending to 600 nm and beyond. Such bands are characteristic for intramolecular CT transitions. Protonation of the dialkylaniline groups in these compounds by treatment of the $CHCl_3$ solutions with a drop of concentrated HCl resulted in a complete loss of the CT transitions (Figure 6) and afforded spectra with longest-wavelength maxima below 500 nm, typical of phenyl (**12**) or 4-nitrophenyl-substituted (**15**) dimers. Treatment of the protonated compounds with aqueous NaOH regenerated the neutral forms with UV/Vis spectra virtually identical to those measured before the treatment with acid. These data show that the dimeric TEE chromophore by itself displays strong

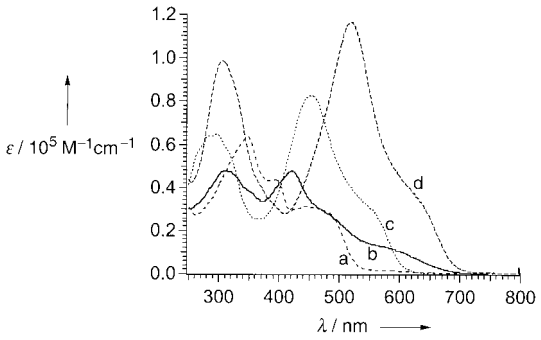

Figure 5. UV/Vis spectra in $CHCl_3$ of **15** (a), **16** (b), **13** (c), and **17** (d) in $CHCl_3$.

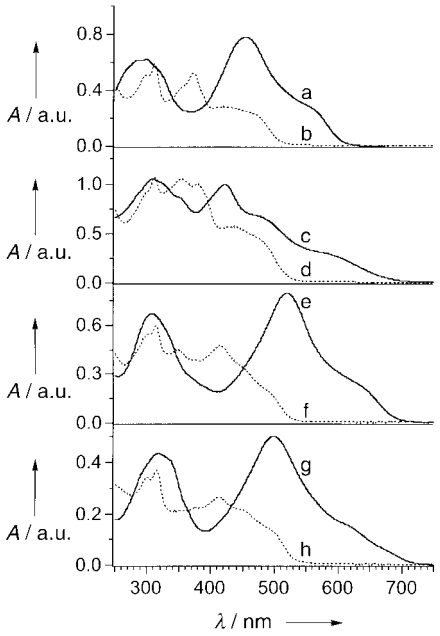

Figure 6. Changes of the UV/Vis absorptions in $CHCl_3$ upon addition of HCl. a) Pure **13** (ca. 9.4×10^{-6} M), b) **13** + HCl, c) pure **16** (ca. 1.9×10^{-5} M), d) **16**+HCl, e) pure **17** (ca. 6.9×10^{-6} M), f) **17**+HCl, g) pure **18** (ca. 4.4×10^{-6} M), h) **18**+HCl.

Table 3. Absorption band maxima and molar extinction coefficients in the UV/Vis spectra of donor/acceptor substituted TEE dimers and expanded radialenes in $CHCl_3$.

Compound	λ_{max} [nm] (ε [$M^{-1}cm^{-1}$])								End-abs. [nm]
12	287 (47300)	301 (*sh*, 41100)	359 (*sh*, 43000)	372 (49500)	390 (49300)	421 (41400)	456 (20200)		530
13	285 (64200)	298 (65100)	453 (82500)	547 (*sh*, 32300)					650
14	301 (60600)	479 (81500)	565 (*sh*, 28400)						650
15	349 (70400)	397 (46300)	446 (31000)	483 (*sh*, 27900)					680
16	304 (54200)	344 (*sh*, 45900)	418 (52600)	477 (*sh*, 37200)	580 (*sh*, 16500)				750
17	304 (97700)	516 (115000)	633 (*sh*, 34100)						740
18	316 (98100)	501 (113000)	616 (*sh*, 37700)						750
25a	297 (148000)	395 (97200)	516 (172000)	646 (171000)					750
25b	301 (111000)	335 (*sh*, 85400)	393 (48100)	429 (*sh*, 56400)	518 (186000)	574 (145000)	609 (*sh*, 114000)	636 (*sh*, 114000)	750
25c	294 (128000)	359 (67700)	517 (234000)	560 (*sh*, 162000)	630 (*sh*, 64400)				750
25d	290 (142000)	307 (140000)	332 (*sh*, 125000)	393 (*sh*, 70700)	514 (232000)	609 (*sh*, 77600)			750
26a	425 (112000)	479 (100000)	536 (109000)	576 (*sh*, 92700)					630
26b	397 (*sh*, 79000)	427 (112000)	504 (189000)						630
26c	396 (*sh*, 103000)	421 (120000)	490 (135000)						630
27b	285 (37400)	298 (37300)	314 (33200)	379 (*sh*, 32900)	399 (37500)	468 (83000)	505 (*sh*, 51100)		575
27d	255 (101000)	294 (97300)	303 (*sh*, 92700)	376 (*sh*, 89100)	389 (104000)	424 (94900)	445 (97300)	499 (*sh*, 60200)	575
27f	263 (142000)	292 (139000)	304 (*sh*, 126000)	373 (*sh*, 125000)	388 (148000)	417 (135000)	445 (126000)	508 (*sh*, 84600)	575

0947-6539/01/0715-3270 $ 17.50+.50/0 *Chem. Eur. J.* **2001**, *7*, No. 15

electron acceptor properties which are enhanced only weakly by the addition of 4-nitrophenyl substituents.

The two additional donor/acceptor substituents in the TEE dimers **13**–**16**, as compared with **6**–**8**,[10b] induce a considerable bathochromic shift of the longest-wavelength absorption maxima, with the effect of the dialkylaniline donor substituents again greatly surpassing the effect of the nitrophenyl acceptor groups. Thus, the longest-wavelength absorption maximum shifts from 456 nm ($\varepsilon = 41\,600\,M^{-1}cm^{-1}$) in the bis(nitrophenyl)-substituted dimer **7** to 483 nm (*sh*, $\varepsilon = 27\,900\,M^{-1}cm^{-1}$) in the tetrakis(nitrophenyl) derivative **15**. Much larger shifts are observed when passing from the diarylated dimers **6** (486 nm, $\varepsilon = 45\,100\,M^{-1}cm^{-1}$) and **8** (481 nm, $\varepsilon = 31\,300\,M^{-1}cm^{-1}$) to the tetraarylated derivatives **13** (547 nm, *sh*, $\varepsilon = 32\,300\,M^{-1}cm^{-1}$) and **16** (580 nm, *sh*, $\varepsilon = 16\,500\,M^{-1}cm^{-1}$), respectively. The smaller shift (27 nm) observed in the comparison between the all-nitrophenyl derivatives (**15** versus **7**) reflects the extension of the overall π-conjugated chromophore, whereas the larger shifts (61 and 99 nm, respectively) seen in the comparison of the dialkylaniline-substituted dimers (**13**, **16** versus **6**, **8**) clearly include contributions from additional intramolecular donor–acceptor conjugation pathways in the molecule.

Further extension of the chromophores in compounds **17** and **18** leads to a significant bathochromic shift of the longest-wavelength absorption band as well as of the optical end-absorption as compared to dimer **14**. Thus, the two additional (4-dialkylaminophenyl)ethynyl residues in **18** generate a bathochromic shift of 51 nm in the maximum of the lowest-energy band and of nearly 100 nm in the optical end-absorption, when compared to **14** (Table 3). In agreement with the findings discussed above, the spectra of **17**, with two additional (4-nitrophenyl)ethynyl acceptor residues, and **18** do not differ much: the longest wavelength absorption maxima differ only by 17 nm and the optical end-absorptions appear at nearly equal wavelength around 740 nm. These data demonstrate that the chromophoric properties of TEE dimers are readily tunable: upon suitable functionalization, their absorption region can be expanded close to the near IR absorption range.

In previous UV/Vis investigations on the per(silylethynylated) expanded [3]-, [4]-, and [5]radialenes **1a**–**c**, we found that the optical end-absorption within the entire macrocyclic series remained almost constant (at ≈485 nm) and appeared bathochromically shifted by only ≈20 nm in comparison to the end-absorption of TEE dimer **9** (at ≈465 nm), a model for the longest linearly conjugated π-electron fragment in the macrocycles, as explained above.[6b] We concluded from these findings, that cross-conjugation in the macrocycles was rather inefficient and that the extent of π-electron delocalization in the expanded radialenes is mainly limited to the longest linearly conjugated π-electron fragment. Further support for such conclusions came from the UV/Vis spectral data in a series of acyclic cross-conjugated chromophores, the per(silylethynylated) expanded dendralenes,[15b] in which π-electron delocalization was also found to extent efficiently only through the longest linearly conjugated fragment.

Upon introduction of dialkylaniline donor groups into the periphery of the electron-accepting perethynylated expanded radialene core in **25a**–**d**, dramatic spectral changes are observed as compared with the series **1a**–**c** bearing lateral silyl groups (Figure 7). Similar to **1a**–**c**, the optical end-absorption in **25a**–**d** occurs at nearly the same wavelength

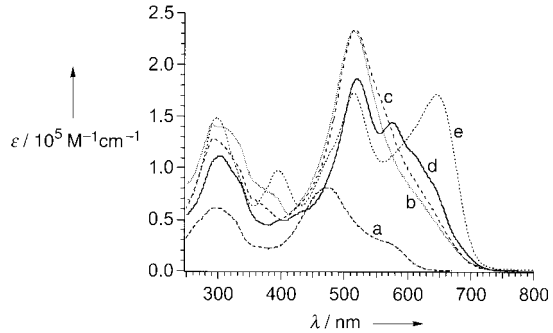

Figure 7. UV/Vis spectra in $CHCl_3$ of TEE dimer **14** (a) and the donor-substituted expanded radialenes **25d** (b), **25c** (c), **25b** (d), and **25a** (e).

around 750 nm. The introduction of the donor groups therefore shifts the end-absorption in **25a**–**d** bathochromically by about 265 nm when compared to **1a**–**c**. When compared to dimer **14**, with an identical longest linearly conjugated π-electron fragment, the absorption onset is shifted bathochromically by about 100 nm. Particularly remarkable is the high intensity longest-wavelength absorption maximum in the spectrum of expanded [3]radialene **25a** ($\lambda_{max} = 646$ nm, $\varepsilon = 171\,000\,M^{-1}cm^{-1}$); at present, we do not have a good explanation for the exceptionally high molar extinction coefficient of this band.

The UV/Vis spectral characteristics of the two other classes of expanded radialenes, **26a**–**c** and **27b**, **d**, **f** (Figure 8) are intermediate between **1a**–**c** with peripheral silyl groups and

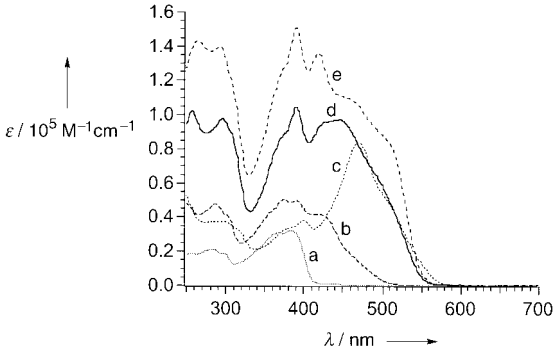

Figure 8. UV/Vis spectra in $CHCl_3$ of **10a** (a), **12** (b), **27b** (c), **27d** (d), and **27f** (e).

25a–**d** with the strong dialkylaniline donor groups (Table 3). Again, the end-absorptions for all members of one series are identical. Changing from **1a**–**c** to **27b**, **d**, **f** with the modest 3,5-di(*tert*-butyl)phenyl donor groups in the periphery, the end-absorption shifts bathochromically by about 90 nm; in comparison to TEE dimer **12**, the absorption onset is shifted by 45 nm. When the strength of the peripheral aryl donor groups is increased in **26a**–**c**, the end-absorption shifts bathochromically by about 145 nm (as compared to **1a**–**c**).

In this series, the expanded [3]radialene **26a** again displays the strongest longest-wavelength absorption maximum.

Both dimeric TEEs and perethynylated expanded radialenes show large bathochromic shifts of their longest wavelength absorption maxima and the absorption onset when their electron acceptor all-carbon cores are laterally functionalized with increasingly strong aryl donor substituents. This is readily explained by enhanced intramolecular charge-transfer interactions. In addition, the investigations comprising four series of compounds clearly demonstrate an additional macrocyclic π-conjugation effect in the perethynylated expanded radialenes, which increases with the strength of the peripheral donors. The comparison with the corresponding dimeric TEEs, featuring the same longest linearly conjugated π-electron fragments, shows bathochromic shifts of the absorption onset of 20 nm (**1a–c** versus **9**), 45 nm (**27b**, **d**, **f** versus **12**), and 100 nm (**25a–d** versus **14**). The differences between absorption onsets correspond to shifts in transition energies of −0.11, −0.18, and −0.25 eV, respectively. These data indicate that macrocyclic cross-conjugation in the expanded radialenes becomes increasingly efficient when going from silyl substituents to electron-donating aryl substituents. The measured bathochromic shifts are more significant than those seen in previous investigations on extended cross-conjugated chromophores; in particular in acyclic systems such as the expanded dendralenes, cross-conjugation effects have been found to be very weak or even non-existing.[15b, 33] We propose that cross-conjugation and homoconjugation-like orbital overlap are more efficient in cyclic than in acyclic π systems as a result of the greater rigidity of the cyclic perimeters. We hope to shed further light on the nature of these donor–acceptor-enhanced macrocyclic π-electron delocalization effects with the help of theoretical calculations.

Electronic emission spectroscopy: The tetrakis(*N*,*N*-dimethylaniline)-substituted TEE dimer **13** displays an intense fluorescence emission in solution, and its maximum was found to be strongly dependent on solvent polarity (Figure 9). In hexane, a dual fluorescence ($\lambda_{max\,em}$ at 565 nm and 604 nm (*sh*); λ_{exc} = 450 nm) was observed whereas in more polar solvents, a single emission band appeared which shifted bathochromically with solvent polarity. These data are reminiscent of the photophysical behavior of *N*,*N*-dimethylaniline-substituted TEE **28**, which also displayed a dual fluorescence in hexane as well as a single, strongly solvent-polarity-dependent emission in more polar solvents. A recent joint experimental and computational study[32e] suggested that this emission behavior of **28** is best rationalized by the TICT (twisted intramolecular charge-transfer) state model, proposed by Grabowski and co-workers to explain the dual fluorescence in organic donor–acceptor compounds.[34, 35] According to this model, the initial excited state reached upon photoexcitation, with a nearly planar chromophore, relaxes to a lower-energy TICT state in which either the dimethylamino or the entire *N*,*N*-dimethylanilino group in **28** takes an orthogonal orientation with respect to the rigid, planar TEE acceptor moiety. A similar mechanism could explain the fluorescence behavior of **13**, and further investigations will be conducted to clarify this interesting phenomenon.

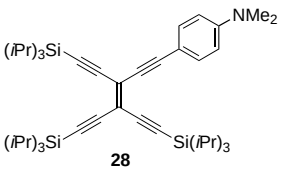

28

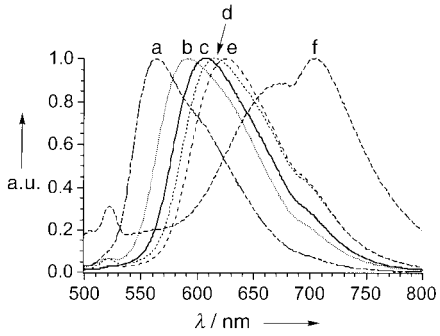

Figure 9. Normalized emission spectra of **13** in different solvents at 20 °C. The emission maxima measured at the excitation wavelength of 450 nm are 565 and 604 nm (*sh*) in hexane (a), 593 nm in Et_2O (b), 609 nm in $CHCl_3$ (c), 616 nm in THF (d), 627 nm in CH_2Cl_2 (e), and 675 nm in CH_3CN (f). The additional peak observed around 705 nm in the more polar solvents (where the fluorescence of **13** becomes weak) is an artifact. [**13**] = 2×10^{-6} M for traces (a–e) and 8×10^{-6} M for trace (f).

Electrochemistry: The redox properties of the new compounds were examined by cyclic (CV) and steady-state (SSV) voltammetry in CH_2Cl_2 with Bu_4NPF_6 (0.1 M) as the supporting electrolyte. The redox potentials (versus Fc/Fc^+ (ferrocene/ferricinium couple)) are reported in Table 4 together—for comparison—with the previously reported data for TEE dimers **6**, **7**,[36] and **9**,[6b] and the expanded radialenes **1a–c**.[6b]

In the series of dimeric TEE derivatives, di(*tert*-butyl)-phenyl-substituted **12** gave a one-electron reduction at −1.50 V occurring on the C_{20} core, as well as an aryl-centered one-electron oxidation at +1.08 V. The corresponding HOMO–LUMO gap is equal to 2.58 eV, which is in good agreement with the HOMO–LUMO gap of 2.7 eV calculated from the longest-wavelength absorption at λ_{max} = 456 nm in the UV/Vis spectrum. TEE dimer **13** is oxidized in two two-electron steps at +0.37 and +0.54 V, centered on its four dimethylanilino groups.[37] The reduction at −1.61 V is a reversible one-electron transfer occurring on the central carbon core; the same reduction potential was measured for TEE dimer **6** bearing two dimethylanilino groups. A similar redox behavior is expectedly found for **14** with four $(H_{25}C_{12})_2NC_6H_4$ groups. The electron-donating dialkylanilino groups present in **13** and **14** make the first reduction more difficult by about 100 mV relative to the dimers **9** and **12**. The push–pull dimer **16** is reduced in two one-electron steps, centered on the two nitrophenyl groups,[37] which potentials (−1.35 and −1.28 V) are separated by 70 mV. Similarly, the oxidation of its two dialkylanilino groups occurs in two distinct one-electron oxidation steps at +0.45 and +0.56 V. In the extended chromophore **17**, the four dialkylanilino groups are oxidized in two two-electron steps, similar to **13**. The reduction of the nitrophenyl groups occurs in one two-electron step at −1.37 V; the peak shape in CV as well as the slope in SSV, however, clearly indicate that the two nitro groups behave as independent redox centers. The second one-

0947-6539/01/0715-3272 $ 17.50+.50/0 *Chem. Eur. J.* **2001**, *7*, No. 15

Table 4. Electrochemical data of TEE dimers and expanded radialenes measured on a glassy carbon electrode in CH_2Cl_2 (if not otherwise stated)+0.1M Bu_4NPF_6. All potentials versus Fc/Fc^+.

Compound	Cyclic voltammetry[a]			Steady state voltammetry	
	E^o[b] [V]	ΔE_p[c] [mV]	E_p[d] [V]	$E_{1/2}$[e] [V]	Slope[f] [mV]
1a[g]	−1.08 (1 e⁻)	61		−1.08	68
	−1.28 (1 e⁻)	73		−1.31	63
1b[g]	−1.35 (1 e⁻)	100		−1.34	83
	−1.64 (1 e⁻)	80		−1.65	69
			−1.94		
1c[g]	−1.27 (2 e⁻)	95		−1.29	72
	−1.67 (1 e⁻)	95		further	
	−1.81(1 e⁻)	95		reductions	
	−1.98 (1 e⁻)	95		not well defined	
6	−1.59 (1 e⁻)	90		−1.61	70
			−1.93	−1.95	84
	+0.47 (2 e⁻)	85		+0.46	82
7	−1.29 (2 e⁻)	75		−1.30	50
	−1.45 (1 e⁻)	70		−1.48	63
	−1.86 (1 e⁻)[h]			−1.88	59
9[g]	−1.52 (1 e⁻)	80		−1.52	70
	−1.89 (1 e⁻)	70		−1.88	60
			−2.90	−2.74	110
12	−1.50 (1 e⁻)	70		−1.51	80
	−1.72 (1 e⁻)	80		−1.75	80
	+1.08 (1 e⁻)	80		+1.10	70
	+1.19 (1 e⁻)	80		+1.20	70
13	−1.61 (1 e⁻)	60		−1.61 (1 e⁻)	60
	−1.90	100			
	+0.37 (2 e⁻)	70		+0.36 (2 e⁻)	60
	+0.54 (2 e⁻)	60		+0.57 (2 e⁻)	60
14	−1.63	91		−1.63 (1 e⁻)	62
	+0.34	70		+0.35 (2 e⁻)	52
	+0.60	83		+0.61 (2 e⁻)	64
16	−1.28 (1 e⁻)	60		−1.31 (2 e⁻)	100
	−1.35 (1 e⁻)	60			
	−1.49 (1 e⁻)	60		−1.50 (1 e⁻)	70
			−2.10		
	+0.45 (1 e⁻)	60		+0.44 (1 e⁻)	60
			+0.56 (1 e⁻)	+0.56 (1 e⁻)	50
17	−1.37 (2 e⁻)	70		−1.38 (2 e⁻)	60
	−1.53 (1 e⁻)	60		−1.54 (1 e⁻)	60
	−1.73 (1 e⁻)	70		−1.77 (1 e⁻)	80
			−2.15		
	+0.36 (2 e⁻)	60		+0.36 (2 e⁻)	60
	+0.57 (2 e⁻)	70		+0.60 (2 e⁻)	60
25a	−1.30 (1 e⁻)	90		−1.31	100
	−1.60 (1 e⁻)	100		−1.64	80
	+0.35 (2 e⁻)	56		+0.32	63
			+0.68	+0.63	120
25b	−1.28 (1 e⁻)	65		−1.31	74
	−1.46 (1 e⁻)	90		−1.50	56
	+0.32 (2 e⁻)	55		+0.32	50
				+0.60	109
				+0.80	122
25c	−1.37 (1 e⁻)	60		−1.39	80
	−1.50 (1 e⁻)	60		−1.52	57
			−1.71		
	+0.30 (2 e⁻)	65		+0.30	65
	+0.61 (2 e⁻)	126		+0.70	128
27b	−1.17 (1 e⁻)	70		−1.17	60
	−1.33 (1 e⁻)	70		−1.33	60
	−1.71 (1 e⁻)	70		−1.73	75
			+1.00 (1 e⁻)	+0.99	80
27d	−1.29 (2 e⁻)	140		−1.30	110
	−1.52 (1 e⁻)	70		−1.53	70
	−1.68 (1 e⁻)	70		−1.69	70
	−1.84 (1 e⁻)	80		−1.88	75
			+1.02	+1.05	75

[a] Scan rate 0.1 $V s^{-1}$. [b] $E^o = (E_{pa}+E_{pc})/2$. [c] $\Delta E_p = E_{ox} - E_{red}$, where subscripts ox and red refer to the conjugated oxidation and reduction steps, respectively. [d] Peak potential E_p for irreversible electron transfer. [e] Half-wave potential $E_{1/2}$. [f] Slope of the linearized plot of E versus $\log [I/(I_{lim} - I)]$. [g] Solvent: THF; ref. [6b]. [h] Reversible at scan rate $> 1\ V s^{-1}$.

electron reduction occurs at −1.53 V on the central carbon core.

The expanded radialenes **25a–c** each underwent two reversible one-electron reductions with an additional third irreversible reduction step being observed for the largest derivative, [5]radialene **25c**. These macrocycles also undergo reversible oxidation steps centered on the dialkylanilino groups; the potentials are in the expected range.[37] The expanded [4]radialene **27b** underwent three well-defined reduction steps, each one being a reversible one-electron transfer, and one oxidation step close to the electrolyte discharge. The expanded [6]radialene **27d** gave four reduction steps as well as one oxidation step also close to the electrolyte discharge. The first reduction peak current for **27d** is about twice the peak current of the forthcoming reduction steps, and the peak potential difference observed by CV at a scan rate of 0.1 $V s^{-1}$ was equal to 140 mV for the first reduction but only 70 mV for the second and third reduction steps. Analysis of the peak characteristics of the first reduction step in the cyclic voltammogram clearly confirmed that this step involves in fact two overlapping reversible one-electron steps whose redox potentials are separated by 80 mV. The corresponding reduction potentials are −1.25 and −1.33 V, respectively. The two separate electron transfers may occur on two opposite "edges" of the [6]radialene which are far away from each other. A similar behavior was recently observed in cobalt grids, in which the first reduction involved two one-electron steps, only separated by 40 mV, and occurring on two ligands on opposite boundaries of the molecular grid.[38] The reduction steps are centered on the perethynylated carbon cores whereas the oxidation step is presumably centered on a di(*tert*-butyl)phenyl group.

No significant difference between the first reduction potential of expanded [4]radialenes **1a** and **27b**, nor between expanded [6]radialenes **1c** and **27d**, was observed. However, the macrocyclic perimeters of the expanded [4]radialenes are much more readily reduced in the first one-electron reduction step which may indicate that the conformations of these radialenes are closer to planarity. The expanded radialenes **25a–c** are more difficult to reduce owing to the electron-donating dialkylanilino substituents. Nevertheless, the reduction of the macrocyclic perimeters remains greatly facilitated relative to the comparison TEE dimers in all three series. Thus, large anodic shifts in the first reduction potential are observed: +170–440 mV for **1a–c** relative to **9**, +210–330 mV for **27b/d** relative to **12**, and +240–320 mV for **25a–c** relative to **14**. These data clearly indicate an increased capacity of the cyclic π-conjugated systems to stabilize radical anions formed upon electron uptake. This effect can be understood by the valence-bond description of cross-conjugation. Thus, charged resonance formulas in which the cyclic perimeter contains $4n+2$ electrons in a cyclic conjugation array can be drawn for both the neutral and reduced macrocycle. However, such formulas are likely to contribute more to the overall resonance hybrid in the reduced compounds. Thus, the supposedly planar expanded [3]- and [4]radialenes should gain a certain degree of aromaticity in the Hückel sense. The linear TEE dimers cannot benefit in the same way upon reduction. It is not straightforward to draw

conclusions from these data with regard to the degree of macrocyclic cross-conjugation in the neutral compounds, as was suggested in the previous reports.[6, 12] A more detailed discussion and understanding of these effects will require high-level theoretical calculations.

Nonlinear optical properties: To investigate the NLO properties, third-harmonic generation[39] (THG) measurements were performed and the second hyperpolarizabilities γ determined (Table 5). All measurements were calibrated against fused silica as the reference using $\chi^{(3)}_{fs} = 1.62 \times 10^{-22}$ m^2 V^{-2} (1.16×10^{-14} esu).[40] The introduction of additional donor or donor and acceptor groups in the tetrakis-arylated dimers **13** and **16** leads to a pronounced increase in the second hyperpolarizability when compared to the bis-arylated derivatives **6** and **8**.[9a] The γ values of the expanded radialenes **25a** and **25b** are huge compared with the values measured for the dimeric TEEs. Even the calculated macroscopic third-order nonlinear susceptibility $\chi^{(3)}_{100\%}$, which expresses the nonlinearity per unit volume, yields an increase of about one order of magnitude. The two expanded radialenes, however, are strongly absorbing at the third-harmonic frequency (700 nm). This affords resonantly enhanced γ values, and comparisons with other materials are therefore difficult without an appropriate dispersion model. Resonance enhancement, although to a much lesser extent, also occurred with some of the dimeric TEE derivatives at a higher fundamental wavelength ($\lambda = 2.1$ μm); most of them were investigated at a lower fundamental wavelength ($\lambda =$ 1.907 μm).

Table 5. Results of the third harmonic generation (THG) experiments.[a]

Compound	ε[b] [M^{-1} cm^{-1}]	γ [10^{-36} esu]	γ [10^{-48} m^{5}V^{-2}]	$\chi^{(3)}_{100\%}/\chi^{(3)}_{fs}$	$\chi^{(3)}_{100\%}$ [10^{-20} m^{2}V^{-2}]
6[c, e]	220	780	11	190	3.1
7[c, e]	0	220	3.0	52	0.8
8[c, e]	0	1500	20	350	5.7
13[c]	230	2036	28	519	8.3
14[d, e]	0	1200	16	140	2.2
16[c]	5900	2243	31	570	9.1
25a[d, e]	27300	18000	250	2700	43
25b[d, e]	12400	7000	98	800	13

[a] $\chi^{(3)}_{100\%}$ was measured relative to $\chi^{(3)}$ of fused silica (fs), for which a value of $\chi^{(3)}_{fs} = 1.6 \times 10^{-22}$ m^{2}V^{-2} (1.16×10^{-14} esu) was used. Experimental error: 10%. $\chi^{(3)}_{100\%}/\chi^{(3)}_{fs}$ and $\chi^{(3)}_{100\%}$ were calculated using the refractive indices and the density of the solvent $CHCl_3$. This gives a lower limit of $\chi^{(3)}_{100\%}$ and is consistent with our previous publications.[9] [b] Molar extinction coefficient at the third harmonic wavelength. [c] THG experiments at a wavelength of 1.907 μm; third harmonic wavelength: 636 nm. [d] THG experiments at a wavelength of 2.1 μm; third harmonic wavelength: 700 nm. [e] Adjusted values from refs. [9a] and [12], where a value of $\chi^{(3)}_{fs} = 3.9 \times 10^{-22}$ m^{2}V^{-2} was used (conversion factor: multiplication with 1.6/3.9 = 0.41).

Conclusion

Tetraethynylethene dimers and perethynylated expanded radialenes have been prepared in good yields by oxidative acetylenic coupling under Hay conditions. Two protocols for synthesizing the expanded radialenes were employed: i) cyclization of TEE monomers, allowing isolation of [*n*]radialenes with $n = 3-5$, or ii) cyclization of TEE dimers, allowing isolation of [*n*]radialenes with $n = 4$, 6, or 8. The first X-ray crystal structure of an expanded radialene was obtained, revealing that cyclic hexameric **27d** adopts a nonplanar, "chair-like" conformation. The analysis of electronic properties by UV/Vis spectroscopy led to several fundamental conclusions: i) Donor or donor–acceptor-substituted dimeric TEE derivatives show very strong absorptions extending over the entire UV/Vis region and their longest-wavelength absorption bands have high charge-transfer character. ii) The all-carbon core (C_{20}) of the dimeric TEEs displays strong electron acceptor properties that are only weakly enhanced further upon introduction of additional 4-nitrophenyl acceptor groups. iii) Enhancing the number of *N*,*N*-dimethylaniline donor substituents in the dimeric TEE derivatives leads to a large bathochromic shift of both longest-wavelength absorption maxima and absorption onset, as a result of additional intramolecular donor–acceptor conjugation pathways that are created in the molecules. iv) Macrocyclic cross-conjugation is very efficient in expanded radialenes featuring peripheral aryl donor substituents. The measured bathochromic shifts of the absorption onset as a result of this conjugation are much larger than those observed in acyclic cross-conjugated systems. This can be explained by the greater rigidity of the cyclic π perimeters, allowing better cross-conjugative and homoconjugation-like orbital overlap. A dual fluorescence was observed in hexane for the tetrakis(*N*,*N*-dimethylaniline)-substituted dimeric TEE **13**. A large solvent-polarity-dependent Stokes shift of the fluorescence band is measured in more polar solvents, and we tentatively explain this interesting emission behavior with the twisted intramolecular charge-transfer (TICT) state model. Electrochemical measurements show that the expanded radialenes are reduced at anodically shifted potentials relative to the corresponding dimers, that is, the cyclic cross-conjugated cores can better accommodate electrons than their linear counterparts.

This paper clearly demonstrates the importance of developing novel organic structures with extended π chromophores. Physical investigations of these compounds provide fundamental new insight into mechanisms of π-electron delocalization, as shown by the clear demonstration of donor–acceptor-enhanced macrocyclic cross-conjugation effects in this paper. In addition, promising advanced materials properties are created as demonstrated by the huge third-order nonlinear optical coefficients of the donor-substituted perethynylated expanded radialenes **25a**,**b** and by their ability to form monolayers at the air/water interface, described elsewhere.[12]

Experimental Section

Materials and general methods: Chemicals were purchased from Aldrich and Fluka and used as received. THF for use in the Sonogashira couplings was distilled from sodium/benzophenone. All reactions, except from the Hay couplings, were carried out under an inert atmosphere of Ar or N_2 by

0947-6539/01/0715-3274 $ 17.50+.50/0 *Chem. Eur. J.* **2001**, *7*, No. 15

applying a positive pressure of the protecting gas. For the Sonogashira couplings, solvents were vigorously degassed with Ar in an ultra-sonicator bath for at least 30 min. For the Hay couplings, the following mixture was used as "Hay catalyst": CuCl (0.13 g) and *N,N,N′,N′*-tetramethylethylendiamine (TMEDA, 0.16 g) in CH_2Cl_2 (4.5 mL). Evaporation and concentration in vacuo were carried out under water aspirator pressure. Column chromatographic (CC) purification refers to flash chromatography using solvent mixture in the given ratio on silica gel 60 (230–400 mesh) or on SiO_2-H. For preparative thin-layer chromatography, silica gel 60 F_{254} glass plates were employed. Gravity GPC was performed on Biobeads S-X1 and the fractions analyzed by an analytical GPC instrument. Analytical GPC was carried out with Merck Hitachi (LaChrom) equipment (L-7100 pump, L-7360 column oven, L-7400 UV detector) operated at 40 °C with THF as solvent, and a flow rate of 1.0 mL min^{-1}. Melting points (M.p.) were measured on a Büchi 510 melting point apparatus and are uncorrected. ^{1}H and ^{13}C NMR spectra were recorded on a Varian Gemini 200 MHz or a Bruker 500 MHz spectrometer. Chemical shift values are reported in ppm relative to residual solvent peaks. IR spectra [cm^{-1}] were obtained with a Nicolet 600 FT-IR spectrometer; signal designations: s = strong, m = medium, w = weak. UV/Vis measurements {λ_{max} [nm] (ε [M^{-1}cm^{-1}])} were performed on a CARY 5 UV/Vis NIR spectrophotometer. For the electronic emission spectroscopy studies, a Spex 1680 0.22m Double Spectrometer was used. EI mass spectra were recorded on a VG-Tribid instrument and FAB spectra on a VG-ZAB-2SEQ instrument (matrix: 3-nitrobenzyl alcohol). High-resolution (HR) MALDI spectra were measured on an IonSpec Fourier Transform (FT) Instrument, using a two-layer technique (tl), with 2,5-dihydroxybenzoic acid (DHB) in MeOH/H_2O as matrix, and the compound typically dissolved in CH_2Cl_2. MALDI-TOF spectra were recorded on a Bruker Reflex instrument, with the compound dissolved in CH_2Cl_2, and using as matrix either i) α-cyanocinnamic acid (CCA, 0.1M in CH_3CN/EtOH/H_2O 50:45:5), ii) a mixture of 2,4,6-trihydroxyacetophenone (THA, 0.5M in H_2O) and diammonium citrate (0.1M in H_2O), or iii) 3-indoleacrylic acid (IAA, 0.02M in THF). Elementary analyses were done by Mikrolabor des Laboratorium fur Organische Chemie at ETH Zürich.

Electrochemistry: CH_2Cl_2 was purchased spectroscopic grade from Merck, dried over molecular sieves (4 Å), and stored under Ar prior to use. Bu_4NPF_6 was purchased electrochemical grade from Fluka and used as received. The electrochemical experiments were carried out at 20 ± 2° in CH_2Cl_2 containing 0.1M Bu_4NPF_6 in a classical three-electrode cell. The working electrode was a glassy carbon disk electrode (3 mm in diameter) used either motionless for CV (0.1 to 10 V s^{-1}) or as rotating-disk electrode for SSV. The auxiliary electrode was a platinum wire and the pseudo reference electrode used was also a platinum wire. All potentials are referenced to the ferrocene/ferricinium (Fc/Fc^+) couple used as an internal standard. The accessible range of potentials on the glassy carbon electrode was +1.4 to −2.4 V versus Fc/Fc^+ in CH_2Cl_2. The electrochemical cell was connected to a computerized multipurpose electrochemical device AUTOLAB (Eco Chemie BV, Utrecht, The Netherlands) controlled by the GPSE software running on a personal computer.

Third-harmonic generation: The laser source was either a pulsed Nd/YAG laser (λ = 1.064 μm, 10 Hz repetition rate, pulse duration of 5 ns) which was used to pump a H_2 gas Raman cell yielding a frequency shifted wavelength of λ = 1.907 μm, or a pulsed holmium laser (2 Hz, 80 ns, 35 mJ) at the wavelength of λ = 2.1 μm. The *s*-polarized parallel beam was focused onto the sample with a f = 500 mm lens. Third-harmonic generation measurements were performed by rotating the 1 mm or 0.2 mm thick fused silica cuvette with the solution parallel to the polarization to generate well known Maker-fringe interference patterns. The analysis of the Maker-fringe patterns was done as described in the literature.[41] We used $\chi^{(3)}_{fs}$ = 1.62×10^{-22} m^2 V^{-2} (1.16×10^{-14} esu) as reference for the calibration.[40] A comparison of measurements of fused silica in vacuum and air allowed all subsequent measurements to be performed in air. $CHCl_3$ solutions with initial concentrations of 0.5 to 1.5 weight percent were prepared and later diluted to four lower concentrations. From the concentration series, the molecular second hyperpolarizability of the solute molecules was elucidated, and an extrapolation of $\chi^{(3)}_{100\%}$ for the solid state of the molecules, employing the refractive indices and density of $CHCl_3$, was calculated.

X-ray crystallography

X-ray crystal structure of 13: Single crystals were grown by slow evaporation of a CH_2Cl_2/CH_3CN solution at room temperature. Crystal size: 0.1 × 0.1 × 0.1 mm. X-ray crystal data for $C_{70}H_{82}N_4Si_2$ (M_r = 1035.6): orthorhombic, space group *Pbca*, ρ_{calcd} = 1.092 g cm^{-3}, Z = 4, a = 15.947(11), b = 16.133(10), c = 24.494(15) Å, V = 6302(7) Å^3. Data were collected on a SYNTEX P21 diffractometer, $Mo_{K\alpha}$ radiation, $3 \le 2\theta \le 40°$, 2939 unique reflections, T = 293 K. The structure was solved by direct methods (SHELXTL PLUS)[42] and refined by full-matrix least-squares analysis using experimental weights (heavy atoms anisotropic, H atoms fixed, whereby H positions are based on stereochemical considerations). Final $R(F)$ = 0.057, $wR(F^2)$ = 0.13 for 353 variables and 1893 observed reflections with $I > 2\sigma(I)$.

X-ray crystal structure of 27d: Single crystals were obtained by slow diffusion of hexane into a $CDCl_3$ solution at room temperature. Approximate crystal size: 0.25 × 0.25 × 0.23 mm. X-ray crystal data at 203 K for $(C_{228}H_{252})\cdot(C_6H_{14})$ [M_r = 3078.5]: triclinic, space group $P\bar{1}$ (no. 2), ρ_{calcd} = 0.80 g cm^{-3}, Z = 1, a = 15.833(4), b = 20.110(5), c = 21.655(6) Å, α = 73.33(2), β = 75.43(2), γ = 84.04(2)°, V = 6389(3) Å^3. Data were collected on a Nonius *CAD4* diffractometer, $Cu_{K\alpha}$ radiation, λ = 1.5418 Å. The structure was solved by direct methods (*SIR92*)[43] and refined by full-matrix least-squares analysis (SHELXL-97)[44], using an isotropic extinction correction and $w = 1/[\sigma^2(F_o^2)+(0.160P)^2+5.90P]$, where $P = (F_o^2+2F_c^2)/3$. The $(CH_3)_3C$ groups are highly disordered. For three $(CH_3)_3C$ groups, two orientations were refined isotropically with atomic population parameters (pp) of ½, for four groups two orientations were refined with pp of ⅔ and ⅓, respectively, and for five groups only one orientation was refined anisotropically with pp of 1.0. The disordered $(CH_3)_3C$ groups were restrained to approximately tetrahedral symmetry and C–C bond lengths of about 1.54 Å. In Figure 3a, only one orientation is shown for clarity. The remaining heavy atoms of **27d** were refined anisotropically (H-atoms within the ordered skeleton isotropically, whereby H-positions are based on stereochemical considerations). In addition, a disordered hexane, sitting above the macrocyclic core was also refined anisotropically with pp of 0.5. In the final difference-map, 35 weak electron-density peaks between about 0.6 and 0.9 e Å^{-3} were found in three distinct regions of the asymmetric unit. It is likely that they are due to three highly disordered hexane molecules. They were not refined but included in the structure factor calculation as C atoms with pp between 0.2 and 0.5 (Note that with four hexane molecules in the asymmetric unit, the calculated density would increase from 0.8 to about 1). Final $R(F)$ = 0.136, $wR(F^2)$ = 0.349 for 1082 parameters, 84 restraints and 9518 reflections with $I > 2\sigma(I)$ and $\theta < 50.0°$.

Crystallographic data (excluding structure factors) for the structures reported in this paper have been deposited with the Cambridge Crystallographic Data Centre as supplementary publication no. CCDC-154967 (**13**), 155009 (**27d**). Copies of the data can be obtained free of charge on application to CCDC, 12 Union Road, Cambridge CB2 1EZ, UK (fax: (+44) 1223-336-033; e-mail: deposit@ccdc.cam.ac.uk).

1-[3,5-Di(*tert*-butyl)phenyl]-3-{[3,5-di(*tert*-butyl)phenyl]ethynyl}-4-[(triisopropylsilyl)ethynyl]-6-(trimethylsilyl)hex-3-ene-1,5-diyne (10a): Compounds **5b** (105 mg, 0.227 mmol) and **11** (182 mg, 0.849 mmol) were dissolved in NEt_3 (10 mL) and THF (1 mL), vigorously degassed with Ar. $[PdCl_2(PPh_3)_2]$ (10 mg, 0.014 mmol) and CuI (7 mg, 0.04 mmol) were added under a positive pressure of Ar. The mixture was stirred overnight, whereupon the metal salts were precipitated with hexane and filtered off on Celite. Concentration in vacuo and CC [silica gel; hexanes, then hexanes/CH_2Cl_2 15:1], afforded **10a** (119 mg, 72%) as an orange oil, which turned into a foam upon drying in vacuo. M.p. 45–46 °C; ^{1}H NMR (200 MHz, $CDCl_3$): δ = 7.43–7.46 (m, 2H), 7.38 (d, J = 5.4 Hz, 2H), 7.37 (d, J = 5.8 Hz, 2H), 1.32 (s, 36H), 1.10 (s, 21H), 0.25 (s, 9H); ^{13}C NMR (50 MHz, $CDCl_3$): δ = 150.9, 150.7, 126.2, 126.1, 123.6, 123.4, 121.8, 119.0, 116.0, 104.3, 103.8, 102.2, 102.0, 100.1, 100.0, 86.3, 85.9, 34.8, 31.3, 18.7, 11.4, −0.11; IR (CCl_4): $\tilde{\nu}$ = 2965 (s), 2903 (m), 2866 (m), 2191 (w), 2142 (w), 1588 (m), 1476 (w), 1463 (w), 1431 (w), 1394 (w), 1364 (w), 1259 (w), 1248 (m), 1143 (w), 1045 (w), 1017 (w); UV/Vis ($CHCl_3$): 254 (18300), 275 (*sh*, 19900), 281 (20700), 297 (18400), 365 (30200), 383 (31700); HR-MALDI-MS (DHB-tl): *m/z* (%): calcd for $C_{50}H_{72}Si_2$: 728.5173; found: 728.5178 [M]$^+$, 751.5068 [M+Na]$^+$; elemental analysis calcd (%) for $C_{50}H_{72}Si_2$ (729.29): C 82.35, H 9.95; found: C 82.46, H 9.99.

1-[3,5-Di(*tert*-butyl)phenyl]-3-{[3,5-di(*tert*-butyl)phenyl]ethynyl}-4-[(trimethylsilyl)ethynyl]-6-(trimethylsilyl)hex-3-ene-1,5-diyne (10b): A solution of **5c** (1.80 g, 4.76 mmol) and **11** (1.56 g, 7.29 mmol) in NEt_3 (80 mL) was treated with $[PdCl_2(PPh_3)_2]$ (0.080 g, 0.115 mmol) and CuI (0.040 g, 0.211 mmol). After stirring for 24 h under N_2, the solvent was removed in

vacuo. The brown residue was subjected to CC (SiO_2-H; hexane), affording **10b** (1.70 g, 83%) as an orange solid. M.p. 188–190 °C; ^{1}H NMR (200 MHz, $CDCl_3$): $\delta = 7.43$ (s, 2H), 7.40 (s, 4H), 1.33 (s, 36H), 0.27 (s, 18H); ^{13}C NMR (50 MHz, $CDCl_3$): $\delta = 151.0$, 126.3, 123.7, 121.7, 120.3, 115.7, 104.7, 101.7, 100.4, 86.1, 34.8, 31.3, −0.2; IR (neat): $\tilde{\nu} = 2963$ (s), 2868 (m), 2192 (m), 2143 (m), 1588 (m), 1476 (w), 1430 (w), 1363 (w), 1249 (m), 1142 (w), 1045 (w), 845 (s), 760 (m); UV/Vis ($CHCl_3$): 273 (*sh*, 20200), 283 (21700), 299 (19200), 367 (30200), 386 (30600); EI-MS: *m*/*z* (%): 644 (100) $[M]^+$, 73 (10) $[SiCH_3]^+$; elemental analysis calcd (%) for $C_{44}H_{60}Si_2$ (645.13): C 81.92, H 9.37; found: C 82.06, H 9.36.

1,12-Bis[3,5-di(*tert*-butyl)phenyl]-3,10-bis{[3,5-di(*tert*-butyl)phenyl]ethynyl}-4,9-bis[(triisopropylsilyl)ethynyl]-dodeca-3,9-diene-1,5,7,11-tetrayne (12): A mixture of **10a** (77 mg, 0.11 mmol) and K_2CO_3 (13 mg, 0.094 mmol) in wet MeOH (7 mL) and THF (1.5 mL) was stirred at r.t. for 2 h. Et_2O (100 mL) and H_2O (100 mL) were added, and the organic phase was dried ($MgSO_4$), and concentrated in vacuo. The residue was dissolved in CH_2Cl_2 (10 mL), whereupon Hay catalyst (2.5 mL) was added, and the mixture was stirred under air overnight. Evaporation in vacuo and CC (silica gel; CH_2Cl_2/hexanes 10:1) afforded **12** (42 mg, 61%) as an orange oil, which solidified upon standing. M.p. 93–95 °C; analytical GPC (THF, 40 °C, $\lambda =$ 400 nm): $t_R = 17.0$ min; ^{1}H NMR (200 MHz, $CDCl_3$): $\delta = 7.45$–7.43 (m, 6H), 7.41–7.38 (m, 6H), 1.33 (s, 36H), 1.29 (s, 36H), 1.10/1.09 (2 × s, 42H); ^{13}C NMR (50 MHz, $CDCl_3$): $\delta = 151.2$, 150.9, 126.6, 126.3, 124.0, 123.8, 121.9, 121.6, 121.4, 115.1, 102.9, 102.3, 102.0, 101.7, 86.9, 85.9, 83.6, 82.3, 34.8, 34.7, 31.3, 18.6, 11.2; IR (CCl_4): $\tilde{\nu} = 2965$ (s), 2904 (m), 2866 (s), 2359 (w), 2338 (w), 2184 (m), 2138 (w), 1589 (m), 1464 (m), 1434 (m), 1394 (w), 1363 (m); UV/Vis ($CHCl_3$): 287 (47300), 301 (*sh*, 41100), 359 (*sh*, 43000), 372 (49500), 390 (49300), 421 (41400), 456 (20200); HR-MALDI-MS (DHB-tl): *m*/*z*: calcd for $C_{94}H_{126}Si_2Na$: 1333.9296; found: 1333.9286 $[M+Na]^+$; elemental analysis calcd (%) for $C_{94}H_{126}Si_2$ (1312.20): C 86.04, H 9.68; found: C 86.24, H 9.79.

1,12-Bis[4-(*N*,*N*-dimethylamino)phenyl]-3,10-bis{[4-(*N*,*N*-dimethylamino)-phenyl]ethynyl}-4,9-bis[(triisopropylsilyl)ethynyl]-dodeca-3,9-diene-1,5,7,11-tetrayne (13): A mixture of **2b** (75 mg, 0.13 mmol) and K_2CO_3 (15 mg, 0.11 mmol) in wet MeOH (7.5 mL) and THF (1.5 mL) was stirred at r.t. for 2 h. Et_2O (100 mL) and H_2O (100 mL) were added, and the organic phase was dried ($MgSO_4$) and concentrated in vacuo. The residue was dissolved in CH_2Cl_2 (15 mL), whereupon Hay catalyst (3.5 mL) was added, and the mixture was stirred under air overnight. Evaporation in vacuo and CC (silica gel; CH_2Cl_2/hexanes 2:1) provided **13** (46 mg, 70%) as a dark-red solid. M.p. 204–205 °C; ^{1}H NMR (200 MHz, $CDCl_3$): $\delta = 7.41$ (d, $J =$ 9.0 Hz, 4H), 7.38 (d, $J = 9.0$ Hz, 4H), 6.63 (d, $J = 9.0$ Hz, 4H), 6.51 (d, $J = 9.0$ Hz, 4H), 3.01 (s, 12H), 2.92 (s, 12H), 1.13 (s, 42H); ^{13}C NMR (50 MHz, $CDCl_3$): $\delta = 150.5$ (one coincident peak), 133.6, 133.3, 122.2, 111.5 (2 ×), 111.1, 109.2, 108.9, 103.1, 102.5, 102.4, 100.8, 87.4, 86.9, 84.4, 82.3, 40.1, 40.0, 18.8, 11.4; IR (CCl_4): $\tilde{\nu} = 2962$ (m), 2944 (m), 2863 (m), 2202 (w), 2171 (m), 2134 (w), 1603 (s), 1524 (s), 1445 (w), 1354 (m), 1262 (w), 1190 (w), 1107 (m); UV/Vis ($CHCl_3$): 285 (64200), 298 (65100), 453 (82500), 547 (*sh*, 32300); FAB-MS: *m*/*z*: 1036 $[M+H]^+$; HR-MALDI-MS (DHB-tl): *m*/*z*: calcd for $C_{70}H_{82}N_4Si_2$: 1034.6078; found: 1034.6064 $[M]^+$, 1057.5979 $[M+Na]^+$; X-ray: see Figure 2.

1,12-Bis[4-(*N*,*N*-didodecylamino)phenyl]-3,10-bis{[4-(*N*,*N*-didodecylamino)-phenyl]ethynyl}-4,9-bis[(triisopropylsilyl)ethynyl]-dodeca-3,9-diene-1,5,7,11-tetrayne (14): A mixture of **3b** (36 mg, 0.030 mmol) and K_2CO_3 (30 mg, 0.22 mmol) in MeOH (5 mL), THF (10 mL), and H_2O (ca. five drops) was stirred at r.t. for 12 h. Et_2O (150 mL) was added, and the mixture was washed with H_2O (2 × 200 mL) and sat. aq. NaCl solution (200 mL), dried ($MgSO_4$), and concentrated in vacuo. The residue was dissolved in CH_2Cl_2 (15 mL), whereupon Hay catalyst (0.8 mL) was added. After stirring for 10 h under air, the solvent was removed in vacuo and CC (silica gel; CH_2Cl_2/hexanes 4:1) yielded **14** (29 mg, 86%) as a dark-red oil. ^{1}H NMR (200 MHz, $CDCl_3$): $\delta = 7.35$ (d, $J = 8.9$ Hz, 4H), 7.33 (d, $J =$ 8.9 Hz, 4H), 6.53 (d, $J = 8.9$ Hz, 4H), 6.44 (d, $J = 8.9$ Hz, 4H), 3.31–3.16 (m, 16H), 1.54 (s, 16H), 1.26 (s, 144H), 1.13 (s, 42H), 0.87 (2 × t, $J = 5.6$ Hz, 24H); ^{13}C NMR ($CDCl_3$): $\delta = 148.6$, 133.9, 133.6, 122.5, 111.3, 111.1, 110.5, 108.3, 108.0, 103.5, 102.9, 102.7, 100.3, 87.5, 87.0, 84.6, 82.4, 50.9, 31.9, 29.6, 29.5, 29.3, 29.1, 27.2, 27.1, 22.6, 22.5, 18.7, 18.5, 14.0, 11.3; IR (CCl_4): $\tilde{\nu} = 2958$ (m), 2926 (s), 2854 (m), 2198 (w), 2168 (m), 2133 (w), 1603 (s), 1519 (s), 1465 (w), 1403 (w), 1368 (w), 1260 (w), 1190 (w), 1109 (m), 1074 (w), 1015 (w); UV/Vis ($CHCl_3$): 301 (60600), 479 (81500), 565 (*sh*, 28400); FAB-MS: *m*/*z*: 2267 $[M+H]^+$; elemental analysis calcd (%) for $C_{158}H_{258}N_4Si_2$ (2269.98): C 83.60, H 11.46, N 2.47; found: C 83.49, H 11.27, N 2.22.

1,12-Bis(4-nitrophenyl)-3,10-bis[(4-nitrophenyl)ethynyl]-4,9-bis[(triisopropylsilyl)ethynyl]-dodeca-3,9-diene-1,5,7,11-tetrayne (15): A mixture of **4b** (106 mg, 0.178 mmol) and K_2CO_3 (10 mg, 0.07 mmol) in wet MeOH (5 mL) and THF (5 mL) was stirred at r.t. for 2 h. Et_2O and H_2O were added and the organic phase was dried ($MgSO_4$) and evaporated to 5 mL. CH_2Cl_2 (10 mL) was added, followed by Hay catalyst (2 mL), and the mixture was stirred for 6 h under air. Evaporation in vacuo and CC (SiO_2-H; hexanes/$CHCl_3$ 3:2), afforded **15** (50 mg, 54%) as a dark-orange solid. M.p. 174–176 °C; ^{1}H NMR (200 MHz, $CDCl_3$): $\delta = 8.25$ (d, $J = 8.8$ Hz, 4H), 8.09 (d, $J = 8.8$ Hz, 4H), 7.69 (d, $J = 8.8$ Hz, 4H), 7.62 (d, $J = 8.8$ Hz, 4H), 1.12 (s, 42H); ^{13}C NMR (50 MHz, $CDCl_3$): $\delta = 147.9$ (two peaks), 147.7, 132.7, 128.6, 128.4, 123.7, 119.7, 118.7, 107.0, 101.3, 98.8, 98.0, 91.0, 90.4, 84.2, 83.5, 18.5, 11.0; IR (CCl_4): 2933 (m), 2861 (m), 2189 (w), 2122 (w), 1592 (s), 1517 (s), 1339 (s); UV/Vis ($CHCl_3$): 349 (70400), 397 (46300), 446 (31000), 483 (*sh*, 27900); FAB-MS: *m*/*z*: 1043 $[M+H]^+$; elemental analysis calcd (%) for $C_{62}H_{58}N_4O_8Si_2$: C 71.38, H 5.60, N 5.37; found: C 71.30, H 5.73, N 5.29.

1-[4-(*N*,*N*-dimethylamino)phenyl]-3-{[4-(*N*,*N*-dimethylamino)phenyl]-ethynyl}-12-(4-nitrophenyl)-10-[(4-nitrophenyl)ethynyl]-4,9-bis[(triisopropylsilyl)ethynyl]-dodeca-3,9-diene-1,5,7,11-tetrayne (16): A mixture of **2b** (33 mg, 0.056 mmol), **4b** (34 mg, 0.057 mmol), and K_2CO_3 (14 mg, 0.10 mmol) in wet MeOH (7 mL) and THF (1.5 mL) was stirred at r.t. for 2 h. Et_2O (50 mL) and H_2O (50 mL) were added, and the organic phase was dried ($MgSO_4$) and concentrated in vacuo. The residue was dissolved in CH_2Cl_2 (10 mL), whereupon Hay catalyst (2.7 mL) was added, and the mixture was stirred under air overnight. Evaporation in vacuo and CC (silica gel, CH_2Cl_2/hexanes 2:1) provided a mixture of **13** and **16** (first fraction) and pure **15** (10 mg, 17%) as a dark orange solid. The mixture of **13** and **16** was separated by preparative thin-layer chromatography (silica gel; CH_2Cl_2/hexanes 2:1), affording **13** (12 mg, 21%) as a dark-red solid and **16** (21 mg, 36%) as a dark-brown solid. **16**: M.p. > 250 °C; ^{1}H NMR (200 MHz, $CDCl_3$): $\delta = 8.24$ (d, $J = 9.0$ Hz, 2H), 7.98 (d, $J = 9.0$ Hz, 2H), 7.67 (d, $J = 9.0$ Hz, 2H), 7.54 (d, $J = 9.0$ Hz, 2H), 7.43 (d, $J = 9.0$ Hz, 2H), 7.32 (d, $J = 9.0$ Hz, 2H), 6.64 (d, $J = 9.0$ Hz, 2H), 6.42 (d, $J = 9.0$ Hz, 2H), 3.02 (s, 6H), 2.90 (s, 6H), 1.13 (m, 42H); ^{13}C NMR (125 MHz, $CDCl_3$): $\delta =$ 150.8, 150.5, 147.6, 147.3, 133.5, 132.6, 132.5, 129.0, 128.5, 123.9, 123.6, 123.5, 119.7, 117.8, 111.5 (2 ×), 109.9, 108.9, 108.6, 105.8, 104.2, 103.0, 102.5, 101.9, 101.7, 97.9, 97.7, 91.2, 91.0, 87.6, 87.3, 87.1, 85.7, 82.6, 81.0, 40.1, 39.9, 18.7 (× 2), 11.4, 11.3; IR (CCl_4): $\tilde{\nu} = 2960$ (m), 2946 (m), 2893 (w), 2865 (m), 2201 (w), 2166 (m), 1605 (s), 1524 (s), 1464 (w), 1446 (w), 1343 (s), 1261 (m), 1112 (m), 1072 (m), 1014 (m); UV/Vis ($CHCl_3$): 304 (54200), 344 (*sh*, 45900), 418 (52600), 477 (*sh*, 37200), 580 (*sh*, 16500); HR-MALDI-MS (DHB-tl): *m*/*z*: calcd for $C_{66}H_{70}N_4O_4Si_2$: 1038.4936; found: 1038.4938 $[M]^+$.

1,14-Bis[(4-nitrophenyl)]-5,10-bis{3-[4-(*N*,*N*-didodecylamino)phenyl]-1-[(4-(*N*,*N*-didodecylamino)phenyl)ethynyl]prop-2-ynylidene}tetradeca-1,3,6,8,11,13-hexayne (17): A solution of **14** (25 mg, 0.011 mmol) in THF (16 mL) and H_2O (0.9 mL) was treated with a solution of Bu_4NF in THF (1M, 0.9 mL), and the mixture was stirred overnight at r.t. Et_2O (200 mL) was added, and the organic phase was washed with H_2O (2 × 200 mL), dried ($MgSO_4$), and concentrated in vacuo. The residue was dissolved in CH_2Cl_2 (20 mL), whereupon (4-nitrophenyl)acetylene (19 mg, 0.13 mmol) and Hay catalyst (2.0 mL) were added. The resulting violet mixture was stirred under air for 21 h, then concentrated in vacuo at r.t. CC (silica gel; CH_2Cl_2/hexane 2:3), followed by crystallization (without heating) from CH_2Cl_2/MeOH, gave **17** (16 mg, 65%) as a violet solid. M.p. 77–78 °C; ^{1}H NMR (200 MHz, $CDCl_3$): $\delta = 8.21$ (d, $J = 9.0$ Hz, 4H), 7.66 (d, $J =$ 9.0 Hz, 4H), 7.44 (d, $J = 9.0$ Hz, 4H), 7.38 (d, $J = 9.0$ Hz, 4H), 6.57 (d, $J =$ 9.0 Hz, 4H), 6.47 (d, $J = 9.0$ Hz, 4H), 3.32–3.16 (m, 16H), 1.53 (m, 16H), 1.26 (m, 144H), 0.88/0.87 (2 × t, $J = 6.0$ Hz, 24H); ^{13}C NMR (125 MHz, $CDCl_3$): $\delta = 149.0$ (2 ×), 147.4, 134.2, 134.0, 133.1, 129.1, 125.9, 123.7, 111.3, 111.2, 107.5, 107.3, 106.6, 105.4, 88.2, 87.7, 83.8, 83.3, 83.0, 82.6, 81.2, 79.9, 51.0, 50.9, 31.9 (2 ×), 29.7, 29.6 (2 ×), 29.5, 29.4, 29.3, 27.3, 27.2, 27.1 (× 2), 22.7 (× 2), 14.1; IR (CCl_4): $\tilde{\nu} = 2957$ (m), 2927 (s), 2855 (m), 2162 (s), 1745 (w), 1602 (s), 1522 (s), 1467 (w), 1402 (w), 1368 (m), 1341 (m), 1261 (w), 1216 (w), 1190 (w), 1116 (m); UV/Vis ($CHCl_3$): 304 (97700), 516 (115000), 633 (*sh*, 34100); HR-MALDI-MS (DHB-tl): *m*/*z* (%): calcd for $^{12}C_{155}{}^{13}CH_{224}N_6O_4$: 2246.7543; found: 2246.7604 (30) $[M]^+$, 2269.7452 (100); elemental analysis calcd (%) for $C_{156}H_{224}N_6O_4$ (2247.52): C 83.37, H 10.05, N 3.74; found: C 83.23, H 10.05, N 3.89.

0947-6539/01/0715-3276 $ 17.50+.50/0 *Chem. Eur. J.* **2001**, *7*, No. 15

1,14-Bis[4-(*N*,*N*-didodecylamino)phenyl]-5,10-bis{3-[4-(*N*,*N*-didodecylamino)phenyl]-1-[(4-(*N*,*N*-didodecylamino)phenyl)ethynyl]prop-2-ynylidene}tetradeca-1,3,6,8,11,13-hexayne (18): A solution of **14** (15 mg, 0.0066 mmol) in THF (10 mL) and H_2O (0.5 mL) was treated with a solution of Bu_4NF in THF (1M, 0.6 mL). The mixture was stirred overnight at r.t., whereupon 4-(trimethylsilylethynyl)-(*N*,*N*-didodecylamino)benzene (42 mg, 0.080 mmol) and another portion of Bu_4NF in THF (1M, 0.2 mL) were added. After stirring for 8 h, Et_2O (150 mL) was added and the organic phase was washed with H_2O (2 × 150 mL), dried ($MgSO_4$), and concentrated in vacuo. The residue was dissolved in CH_2Cl_2 (15 mL), whereupon Hay catalyst (ca. 1.2 mL) was added. The resulting violet mixture was stirred under air for 19 h and then concentrated in vacuo at r.t. CC (silica gel; CH_2Cl_2/hexane 1:5 → CH_2Cl_2/hexane 1:1) gave **18** (9 mg, 48%) as an oily solid. ^{1}H NMR (200 MHz, $CDCl_3$): $\delta = 7.45$ (d, $J = 8.6$ Hz, 4H), 7.38 (d, $J = 8.8$ Hz, 4H), 7.37 (d, $J = 8.6$ Hz, 4H), 6.58–6.46 (m, 12H), 3.31–3.16 (m, 24H), 1.54 (s, 24H), 1.26 (br s, 216H), 0.91–0.84 (m, 36H); IR (CCl_4): $\tilde{\nu} = 2959$ (m), 2927 (s), 2855 (m), 2200 (w), 2161 (m), 1745 (w), 1602 (s), 1518 (m), 1467 (w), 1405 (w), 1367 (w), 1262 (m), 1187 (w), 1098 (m), 1017 (m); UV/Vis ($CHCl_3$): 316 (98100), 501 (113000), 616 (*sh*, 37700); HR-MALDI-MS (DHB-tl): *m*/*z* (%): calcd for $^{12}C_{202}{}^{13}C_2H_{324}N_6$: 2860.5605; found: 2860.5906 (66) $[M]^+$, 2883.5723 (100) $[M+Na]^+$.

4-{4-[(11-Bromoundecyl)oxy]phenyl}benzonitrile (20): A solution of **19**[19] (100 mg, 0.274 mmol) and CBr_4 (109 mg, 0.329 mmol) in CH_2Cl_2 (20 mL) was treated with PPh_3 (86.2 mg, 0.329 mmol). After stirring for 2 h at r.t., the solvent was removed in vacuo. The residue was washed with cold MeOH and dried in vacuo, affording **20** (107 mg, 92%). M.p. 77–78 °C; ^{1}H NMR (200 MHz, $CDCl_3$): $\delta = 7.72/7.66$ (2 × d, $J = 8.4$ Hz, 4H), 7.55/7.02 (2 × d, $J = 8.7$ Hz, 4H), 4.03 (t, $J = 6.4$ Hz, 2H), 3.43 (t, $J = 6.9$ Hz, 2H), 2.00–1.80 (m, 4H), 1.60–1.20 (m, 14H); ^{13}C NMR (50 MHz, $CDCl_3$): $\delta =$ 159.9, 145.3, 132.6, 131.3, 128.4, 127.1, 119.1, 115.1, 110.0, 68.1, 33.9, 32.7, 29.4, 29.3, 29.2, 29.1, 28.6, 28.1, 25.9; IR (KBr): $\tilde{\nu} = 2921$ (s), 2848 (s), 2223 (s), 1611 (s), 1473 (s), 1249 (s), 1183 (m), 1038 (m), 834 (s); EI-MS: *m*/*z* (%): 427.2 (32) $[M]^+$, 195.1 (100) $[M-(C_{11}H_{21}Br)]^+$, 178.1 (4) $[M-(C_{11}H_{22}OBr)]^+$; elemental analysis calcd (%) for $C_{24}H_{30}BrNO$ (428.41): C 67.29, H 7.06, N 3.27; found: C 67.30, H 7.22, N 3.11.

4-(4-{[11-(4-Iodophenoxy)undecyl]oxy}phenyl)benzonitrile (21): Compound **20** (100 mg, 0.234 mmol) was added to a solution of 4-iodophenol (50.0 mg, 0.227 mmol) and NaH (22.4 mg, 0.933 mmol) in DMF (10 mL). After stirring for 24 h at r.t., the mixture was poured into cold H_2O. The resulting precipitate was filtered, washed (H_2O), and dried in vacuo, affording **21** (102 mg, 79%). M.p. 114–116 °C; ^{1}H NMR (200 MHz, $CDCl_3$): $\delta = 7.70/7.64$ (2 × d, $J = 8.7$ Hz, 4H), 7.54/7.00 (2 × d, $J = 8.7$ Hz, 4H), 7.54/6.68 (2 × d, $J = 8.7$ Hz, 4H), 4.01 (t, $J = 6.4$ Hz, 2H), 3.92 (t, $J =$ 6.4 Hz, 2H), 1.90–1.70 (m, 4H), 1.60–1.20 (m, 14H); ^{13}C NMR (50 MHz, $CDCl_3$): $\delta = 159.8$, 159.0, 145.2, 138.1, 132.5, 131.2, 128.3, 127.0, 119.1, 116.9, 115.0, 110.0, 82.4, 68.1, 68.0, 29.4, 29.3, 29.2, 29.1, 26.0; IR (KBr): $\tilde{\nu} =$ 2940 (s), 2855 (m), 2223 (m), 1604 (s), 1493 (s), 1473 (s), 1295 (m), 1256 (s), 1177 (s), 828 (s); EI-MS: *m*/*z* (%): 567.1 (92) $[M]^+$, 441.2 (12) $[M-I]^+$, 347.2 (5) $[M-(OC_6H_4I)]^+$, 219.9 (41) $[M-(NC(C_{12}H_8)OC_{11}H_{21})]^+$, 195.0 (100) $[M-(IC_6H_4OC_{11}H_{21})]^+$; HR-EI-MS: *m*/*z*: calcd for $C_{30}H_{34}INO_2$: 567.1634; found: 567.1643 $[M]^+$.

4-{4-[(11-{4-[2-(Triisopropylsilyl)ethynyl]phenoxy}undecyl)oxy]phenyl} benzonitrile (22): Triisopropylsilylacetylene (193 mg, 1.06 mmol), **21** (300 mg, 0.529 mmol), and Bu_4NBr (17.7 mg, 54.9 μmol) were added to a mixture of THF (10 mL) and diisopropylamine (3 mL). The solution was degassed with Ar, whereupon $[PdCl_2(PPh_3)_2]$ (11.5 mg, 16.4 μmol) and CuI (17.7 mg, 92.9 μmol) were added. The mixture was stirred for 2 h at r.t., then the solvent was removed in vacuo and CC (silica gel; CH_2Cl_2/hexane 2:1) gave **22** (315 mg, 96%). M.p. 72–73 °C; ^{1}H NMR (200 MHz, $CDCl_3$): $\delta = 7.70/7.64$ (2 × d, $J = 8.7$ Hz, 4H), 7.54/7.00 (2 × d, $J = 9.1$ Hz, 4H), 7.41/6.82 (2 × d, $J = 9.1$ Hz, 4H), 4.01 (t, $J = 6.2$ Hz, 2H), 3.95 (t, $J = 6.2$ Hz, 2H), 1.87–1.74 (m, 4H), 1.60–1.20 (m, 14H), 1.13 (s, 21H); ^{13}C NMR (50 MHz, $CDCl_3$): $\delta = 159.9$, 159.3, 145.3, 133.5, 133.4, 132.6, 131.3, 128.4, 127.1 (2 ×), 119.1, 115.6, 115.1 (2 ×), 114.4, 110.1, 107.3, 88.5, 68.1, 68.0, 31.5, 29.4, 29.3, 29.1, 25.9, 22.5, 18.6, 11.2; IR (KBr): $\tilde{\nu} = 2940$ (s), 2921 (s), 2861 (s), 2230 (m), 2157 (m), 1611 (s), 1499 (s), 1479 (s), 1289 (s), 1249 (s), 1183 (s), 828 (s); EI-MS: *m*/*z* (%): 621.3 (32) $[M]^+$, 578.3 (100) $[M-(C_3H_7)]^+$; elemental analysis calcd (%) for $C_{41}H_{55}NO_2Si$ (621.98): C 79.18, H 8.91, N 2.25; found: C 78.93, H 8.92, N 2.21.

4-(4-{[11-(4-Ethynylphenoxy)undecyl]oxy}phenyl)benzonitrile (23): A solution of **22** (200 mg, 0.322 mmol) in wet THF was treated with a solution of Bu_4NF in THF (1M, 0.65 mL). After 1 h, TLC (CH_2Cl_2) indicated complete deprotection. The mixture was poured into H_2O and extracted with Et_2O. The organic phase was washed with sat. aq. NaCl solution and H_2O, dried ($MgSO_4$), and concentrated in vacuo. CC (silica gel; CH_2Cl_2) gave **23** (140 mg, 93%) which was used without further purification due to instability. M.p. 97–99 °C; ^{1}H NMR (200 MHz, $CDCl_3$): $\delta = 7.70/7.64$ (2 × d, $J = 8.7$ Hz, 4H), 7.53/7.00 (2 × d, $J = 8.7$ Hz, 4H), 7.42/6.83 (2 × d, $J =$ 8.7 Hz, 4H), 4.01 (t, $J = 6.6$ Hz, 2H), 3.96 (t, $J = 6.6$ Hz, 2H), 2.99 (s, 1H), 1.90–1.70 (m, 4H), 1.52–1.30 (m, 14H); ^{13}C NMR (50 MHz, $CDCl_3$): $\delta =$ 159.8, 159.5, 145.3, 133.5, 132.5, 131.2, 128.3, 127.0, 119.1, 115.1, 114.4, 113.9, 110.0, 83.7, 75.7, 68.0, 29.5, 29.3, 29.1, 26.0.

4,4′-{1-[2-(Triisopropylsilyl)ethynyl]-3-(triisopropylsilyl)prop-2-ynylidene]-methylenebis[ethyne-1,2-diyl-4-phenyleneoxyundecamethylenoxy(4-phenylene)]}dibenzonitrile (24): Compounds **5a** (160 mg, 0.298 mmol) and **23** (601 mg, 1.29 mmol) together with Bu_4NBr (10.0 mg, 0.0310 mmol) were added to a mixture of THF (15 mL) and diisopropylamine (5 mL). The solution was degassed with Ar, whereupon $[PdCl_2(PPh_3)_2]$ (6.40 mg, 9.12 μmol) and CuI (10.0 mg, 52.5 μmol) were added. The mixture was stirred for 2 h at r.t. and subsequently evaporated in vacuo. CC (silica gel; CH_2Cl_2/hexane 1:1) gave **24** (330 mg, 84%); ^{1}H NMR (400 MHz, $CDCl_3$): $\delta = 7.68/7.63$ (2 × d, $J = 8.7$ Hz, 8H), 7.52/6.99 (2 × d, $J = 8.8$ Hz, 8H), 7.43/6.83 (2 × d, $J = 8.9$ Hz, 8H), 4.00 (t, $J = 6.6$ Hz, 4H), 3.97 (t, $J = 6.6$ Hz, 4H), 1.84–1.74 (m, 8H), 1.52–1.40 (m, 8H), 1.40–1.25 (m, 20H), 1.11 (s, 42H); ^{13}C NMR (100 MHz, $CDCl_3$): $\delta = 159.8$, 159.7, 159.6, 145.3, 133.4, 133.3, 132.5, 131.2, 128.3, 127.0, 119.8, 118.2, 115.5, 115.1, 114.7, 114.6, 114.5, 114.4 (×2), 110.0, 104.3, 101.1, 98.8, 86.3, 68.2, 68.1, 29.5 (3 ×), 29.4, 29.3, 29.2, 29.1, 26.0 (2 ×), 18.6, 11.3; IR (KBr): $\tilde{\nu} = 2940$ (s), 2927 (s), 2868 (m), 2223 (w), 2190 (w), 2138 (w), 1604 (s), 1512 (s), 1256 (s); FAB-MS: *m*/*z* (%): 1315.5 (100) $[M+H]^+$, 1271.5 (94) $[M-(C_3H_7)]^+$; elemental analysis calcd (%) for $C_{88}H_{110}N_2O_4Si_2$ (1316.02): C 80.32, H 8.42, N 2.13; found: C 80.04, H 8.52, N 2.10.

5,10,15-Tris{3-[4-(*N*,*N*-didodecylamino)phenyl]-1-[(4-(*N*,*N*-didodecylamino)phenyl)ethynyl]-prop-2-ynylidene}cyclopentadeca-1,3,6,8,11,13-hexayne (25a), **5,10,15,20-tetrakis{3-[4-(*N*,*N*-didodecylamino)phenyl]-1-[(4-(*N*,*N*-didodecylamino)phenyl)ethynyl]prop-2-ynylidene}cycloicosa-1,3,6,8,11,13,16,18-octayne (25b)** and **5,10,15,20,25-pentakis{3-[4-(*N*,*N*-didodecylamino)phenyl]-1-[(4-(*N*,*N*-didodecylamino)phenyl)ethynyl]prop-2-ynylidene}cyclopentacosa-1,3,6,8,11,13,16,18,21,23-decayne (25c)**: A solution of **3a** (0.367 g, 0.284 mmol) in THF (30 mL) was treated with a solution of Bu_4NF in THF (1M, 0.85 mL, 0.85 mmol). After stirring for 24 h, Et_2O (150 mL) was added. The mixture was washed with H_2O (4 × 30 mL) and sat. aq. NaCl solution (30 mL). The organic phase was dried ($MgSO_4$), then reduced to 3 mL. The deprotected TEE was purified by filtration over a short plug (silica gel; CH_2Cl_2), the product fraction was reduced to 10 mL, then treated with a solution of CuCl (0.006 g, 0.061 mmol) and TMEDA (0.03 mL, 0.202 mmol) in CH_2Cl_2 (10 mL). The mixture was stirred for 4 h and then concentrated in vacuo. CC (silica gel; hexane/CH_2Cl_2 3:1) provided **25a** (0.0011 g, 8%), **25b** (0.0043 g, 10%), and **25c** (0.0032 g, 2%). **25a**: Blue oil. $R_f \approx 0.5$ (silica gel; hexane/CH_2Cl_2 3:1); ^{1}H NMR (500 MHz, $CDCl_3$): $\delta = 7.41$ (d, $J = 9.0$ Hz, 12H), 6.56 (d, $J = 9.0$ Hz, 12H), 3.27 (t, $J =$ 8.0 Hz, 24H), 1.57 (m, 24H), 1.27 (m, 216H), 0.89 (t, $J = 7.0$ Hz, 36H); ^{13}C NMR (125 MHz, $CDCl_3$): $\delta = 148.7$, 133.3, 113.4, 111.2, 107.8, 103.4, 98.5, 87.4, 84.9, 51.0, 31.9, 29.8, 29.7, 29.6, 29.5, 29.4, 28.9, 27.3, 27.1, 22.7, 14.1; IR (KBr): $\tilde{\nu} = 2924$ (s), 2853 (m), 2192 (w), 2161 (w), 1602 (m), 1522 (w), 1466 (w), 1406 (w), 1364 (w), 1188 (w), 1125 (m); UV/Vis ($CHCl_3$): 297 (148000), 395 (97200), 516 (172000), 646 (171000); MALDI-TOF-MS (CCA): *m*/*z* (%): calcd for $^{12}C_{208}{}^{13}C_2H_{324}N_6$: 2932.6; found: 5860 (17) $[2M]^+$, 2930 (100) $[M]^+$; **25b**: blue-violet oil. $R_f \approx 0.5$ (silica gel; hexane/CH_2Cl_2 3:1); ^{1}H NMR (500 MHz, $CDCl_3$): $\delta =$ 7.40 (d, $J = 9.0$ Hz, 16H), 6.41 (d, $J = 9.0$ Hz, 16H), 3.15 (t, $J = 8.0$ Hz, 32H), 1.54 (m, 32H), 1.27 (m, 288H), 0.89 (t, $J = 7.0$ Hz, 48H); ^{13}C NMR (125 MHz, $CDCl_3$): $\delta = 148.6$, 133.9, 118.7, 111.2, 110.2, 108.0, 104.5, 87.9, 87.5, 83.9, 53.4, 50.9, 31.9, 31.6, 29.8, 29.7, 29.6, 29.4 (2 ×), 27.3, 27.2, 27.1, 22.7, 22.6, 14.1; IR (KBr): $\tilde{\nu} = 2922$ (s), 2856 (m), 2200 (w), 2156 (s), 1600 (s), 1522 (s), 1367 (m), 1128 (m); UV/Vis ($CHCl_3$): 301 (111000), 335 (*sh*, 85400), 393 (48100), 429 (*sh*, 56400), 518 (186000), 574 (145000), 609 (*sh*, 114000), 636 (*sh*, 114000); MALDI-TOF-MS (CCA): *m*/*z* (%): calcd for $^{12}C_{277}{}^{13}C_3H_{432}N_8$: 3910.4; found: 7812 (12) $[2M]^+$, 3908 (100) $[M]^+$; **25c**: violet oil; $R_f \approx 0.2$ (silica gel; hexane/CH_2Cl_2 3:1); ^{1}H NMR (200 MHz, $CDCl_3$): $\delta = 7.33$ (d, $J = 9.0$ Hz, 20H), 6.31 (d, $J = 9.0$ Hz, 20H), 3.13 (m, 40H), 1.55 (m, 40H), 1.25 (m, 360H), 0.88 (t, $J = 7.0$, 60H); ^{13}C NMR (125 MHz, $CDCl_3$): $\delta = 148.5$, 133.9, 121.6,

111.2, 109.5, 107.8, 104.6, 88.0, 84.5, 83.3, 50.8, 31.9, 29.8, 29.7, 29.6, 29.5, 29.4, 27.2, 27.1, 22.7, 14.1; IR (KBr): $\tilde{\nu}$ = 2924 (s), 2850 (m), 2194 (w), 2156 (m), 1600 (s), 1519 (s); UV/Vis ($CHCl_3$): 294 (128000), 359 (67700), 517 (234000), 560 (*sh*, 162000), 630 (*sh*, 64400); MALDI-TOF-MS (CCA): *m*/*z* (%): calcd for $^{12}C_{347}{}^{13}C_3H_{540}N_{10}$: 4887.3; found: 9778 (6) $[2M]^+$, 4888 (27) $[M]^+$, 2269 (100); elemental analysis calcd (%) for $C_{350}H_{540}N_{10}$ (4888.18): C 86.00, H 11.13, N 2.87; found: C 86.03, H 11.04, N 2.65.

5,10,15,20-Tetrakis{3-[4-(*N*,*N*-didodecylamino)phenyl]-1-[(4-(*N*,*N*-didodecylamino)phenyl)ethynyl]prop-2-ynylidene}cycloicosa-1,3,6,8,11,13,16,18-octayne (25b) and 5,10,15,20,25,30-Hexakis{3-[4-(*N*,*N*-didodecylamino)-phenyl]-1-[(4-(*N*,*N*-didodecylamino)phenyl)ethynyl]prop-2-ynylidene}cyclotriaconta-1,3,6,8,11,13,16,18,21,23,26,28-dodecayne (25d): A solution of **14** (0.028 g, 0.022 mmol) in THF (5 mL) was treated with a solution of Bu_4NF in THF (1M, 0.10 mL, 0.10 mmol). After stirring for 24 at. r.t., Et_2O (150 mL) was added and the mixture was extracted with H_2O (4 × 30 mL) and sat. aq. NaCl solution (30 mL). The organic phase was dried ($MgSO_4$), reduced to 3 mL, and the deprotected compound purified by chromatography on a short silica gel column (CH_2Cl_2). The product fraction was reduced to 20 mL and then treated with a solution of CuCl (0.060 g, 0.612 mmol) and TMEDA (0.4 mL, 2.69 mmol) in CH_2Cl_2 (50 mL). The mixture was stirred for 6 h at r.t., whereupon the solvent was removed in vacuo. CC (silica gel; hexane/CH_2Cl_2 2:1), yielded **25b** (0.003 g, 11%) and **25d** (0.001 g, 3%). **25b**: Blue oil. $R_f \approx 0.6$ (silica gel; hexane/CH_2Cl_2 2:1); spectral data as given above; **25d**: red-violet oil. $R_f = 0.3$ (silica gel; hexane/CH_2Cl_2 2:1); ^{1}H NMR (500 MHz): δ = 7.28 (d, J = 9.0 Hz, 24H), 6.30 (d, J = 9.0 Hz, 24H), 3.10 (m, 48H), 1.52 (m, 48H), 1.25 (m, 432H), 0.86 (t, J = 6.9 Hz, 72H); IR (KBr): $\tilde{\nu}$ = 2924 (s), 2852 (m), 2192 (w), 2157 (m), 1601 (m), 1522 (w), 1364 (w), 1189 (w), 1123 (w), 1086 (w); UV/Vis ($CHCl_3$): 290 (142000), 307 (140000), 332 (*sh*, 125000), 393 (*sh*, 70700), 514 (232000), 609 (*sh*, 77600); MALDI-TOF-MS (CCA): *m*/*z*: calcd for $^{12}C_{416}{}^{13}C_4H_{648}N_{12}$: 5865.1; found: 5859 $[M]^+$.

5,10,15-Tris{3-(4-{11-[4-(4-cyanophenyl)phenoxy]undecyloxy}phenyl)-1-[2-(4-{11-[4-(4-cyanophenyl)phenoxy]undecyloxy}phenyl)ethynyl]prop-2-ynylidene}cyclopentadeca-1,3,6,8,11,13-hexayne (26a), **5,10,15,20-tetrakis{3-(4-{11-[4-(4-cyanophenyl)phenoxy]undecyloxy}phenyl)-1-[2-(4-{11-[4-(4-cyanophenyl)phenoxy]undecyloxy}phenyl)ethynyl]prop-2-ynylidene}cycloicosa-1,3,6,8,11,13,16,18-octayne (26b)** and **5,10,15,20,25-pentakis{3-(4-{11-[4-(4-cyanophenyl)phenoxy]undecyloxy}phenyl)-1-[2-(4-{11-[4-(4-cyanophenyl)phenoxy]undecyloxy}phenyl)ethynyl]prop-2-ynylidene}cyclopentacosa-1,3,6,8,11,13,16,18,21,23-decayne (26c)**: A solution of **24** (300 mg, 0.228 mmol) in wet THF (15 mL) was treated with a solution of Bu_4NF in THF (1M, 1.15 mL). After 1 h, TLC (silica gel; CH_2Cl_2/hexane 2:1) indicated complete deprotection. The mixture was poured into water and then extracted with CH_2Cl_2 (4 × 50 mL). The combined organic phases were washed with sat. aq. NH_4Cl solution (2 × 50 mL) and H_2O, dried ($MgSO_4$), and concentrated in vacuo. CC (silica gel; CH_2Cl_2) gave the bis-deprotected TEE (188 mg, 82%), which was used without further purification due to instability. ^{1}H NMR (200 MHz, $CDCl_3$): δ = 7.69/7.63 (d, J = 8.7 Hz, 8H), 7.52/6.99 (d, J = 9.1 Hz, 8H), 7.47/6.86 (d, J = 9.1 Hz, 8H), 4.00 (t, J = 6.6 Hz, 4H), 3.97 (t, J = 6.6 Hz, 4H), 3.61 (s, 2H), 1.90–1.70 (m, 8H), 1.50–1.25 (m, 28H). A solution of this compound (72.0 mg, 71.8 μmol) in dry benzene (10 mL) was treated with a solution of $Cu(OAc)_2$ (130 mg, 0.716 mmol) in pyridine/benzene (3:1, 30 mL). After stirring for 24 h under air at r.t., a 30% aq. $CuSO_4$ solution was added. The mixture was extracted with CH_2Cl_2, the organic phase was washed with 5% aq. NH_4OH solution and dried ($MgSO_4$). Gravity GPC (CH_2Cl_2) gave **26a**, **26b**, and **26c** as deep-reddish-brown solids. **26a**: Yield: 3 mg (4%); analytical GPC (THF, 40 °C, λ = 400 nm): t_R = 12.23 min; ^{1}H NMR (200 MHz, $CDCl_3$): δ = 7.68/7.62 (2 × d, J = 8.7 Hz, 24H), 7.52/6.98 (2 × d, J = 8.7 Hz, 24H), 7.49/6.87 (2 × d, J = 8.7 Hz, 24H), 3.99 (t, J = 6.6 Hz, 24H), 1.90–1.70 (m, 24H), 1.50–1.25 (m, 84H); UV/Vis ($CHCl_3$): 425 (112000), 479 (100000), 536 (109000), 576 (*sh*, 92700); MALDI-TOF-MS (IAA, negative ion mode): *m*/*z*: calcd for $^{12}C_{208}{}^{13}C_2H_{204}N_6O_{12}$: 3003.6; found: 3003.4 $[M]^-$; **26b**: yield: 40 mg (56%); analytical GPC (THF, 40 °C, λ = 400 nm): t_R = 11.96 min; ^{1}H NMR (200 MHz, $CDCl_3$): δ = 7.68/7.62 (2 × d, J = 8.7 Hz, 32H), 7.51/6.98 (2 × d, J = 8.7 Hz, 32H), 7.47/6.76 (2 × d, J = 8.7 Hz, 32H), 3.99 (t, J = 6.6 Hz, 16H), 3.89 (t, J = 6.6 Hz, 16H), 1.90–1.65 (m, 32H), 1.60–1.20 (m, 112H); ^{13}C NMR (50 MHz, $CDCl_3$): δ = 160.5, 159.9, 145.3, 134.0, 132.6, 131.3, 128.4, 127.1, 119.2, 118.9, 115.1, 114.8, 113.9, 113.0, 110.1, 102.8, 87.0, 86.8, 84.1, 68.1, 29.5, 29.3 (2 ×), 29.1 (2 ×), 26.0, 25.9; IR (KBr): $\tilde{\nu}$ = 2927 (s), 2855 (m), 2230 (w), 2177 (m), 1604 (s), 1519 (s), 1295 (m), 1256 (s), 1177 (m); UV/Vis ($CHCl_3$): 397 (*sh*, 79000), 427 (112000), 504 (189000); MALDI-TOF-MS (IAA, negative ion mode): *m*/*z*: calcd for $^{12}C_{277}{}^{13}C_3H_{272}N_8O_{16}$: 4005.1; found: 4004.3 $[M]^-$; **26c**: yield: 3 mg (4%); analytical GPC (THF, 40 °C, λ = 400 nm): t_R = 11.78 min; ^{1}H NMR (200 MHz, $CDCl_3$): δ = 7.67/7.62 (2 × d, J = 8.3 Hz, 40H), 7.51/6.97 (2 × d, J = 8.7 Hz, 40H), 7.39/6.60 (2 × d, J = 8.7 Hz, 40H), 3.99 (t, J = 6.2 Hz, 20H), 3.77 (t, J = 6.2 Hz, 20H), 1.90–1.65 (m, 40H), 1.50–1.20 (m, 140H); UV/Vis ($CHCl_3$): 396 (*sh*, 103000), 421 (120000), 490 (135000); MALDI-TOF-MS (IAA, negative ion mode): *m*/*z*: calcd for $^{12}C_{346}{}^{13}C_4H_{340}N_{10}O_{20}$: 5006.6; found: 5007.9 $[M]^-$.

Radialenes 27a–f: A solution of **10b** (0.100 g, 0.155 mmol) in THF (5 mL) was treated with a solution of Bu_4NF in THF (1M, 0.80 mL, 0.80 mmol). After stirring for 5 min at r.t., Et_2O (150 mL) was added and the mixture was washed with H_2O (4 × 30 mL) and sat. aq. NaCl solution (30 mL). The organic phase was dried ($MgSO_4$) and then concentrated in vacuo. The residue was filtered through a column (silica gel; hexane/CH_2Cl_2 2:1). The solvent was removed and the resulting white solid redissolved in CH_2Cl_2 (100 mL). A solution of CuCl (0.060 g, 0.612 mmol) and TMEDA (0.4 mL, 2.69 mmol) in CH_2Cl_2 (50 mL) was added, and the mixture was stirred for 2 h at r.t. The solvent was removed in vacuo and the residue purified on a short column (silica gel; hexane/CH_2Cl_2 2:1), affording a mixture of the expanded radialenes **27a–f** (0.018 g, 23%) as a red solid. ^{1}H NMR (200 MHz, $CDCl_3$): δ = 7.35–7.44 (m), 1.29 (s), 1.24 (s), 1.19 (s), 1.17 (s); IR (KBr): $\tilde{\nu}$ = 2963 (s), 2868 (w), 2180 (m), 1589 (m), 1466 (w), 1431 (w), 1363 (m), 1247 (w), 1101 (w), 877 (m); UV/Vis ($CHCl_3$): 257 (21700), 296 (22200), 306 (*sh*, 20600), 374 (*sh*, 20700), 391 (24200), 423 (20600), 462 (22500), 509 (*sh*, 14700) [extinction coefficients calculated per one unit of TEE]; MALDI-TOF-MS (CCA, negative ion mode): *m*/*z* (%): 4977 (1) $[M]^-$ ([10]radialene), 4482 (0.2) $[M]^-$ ([9]radialene), 3980 (2) $[M]^-$ ([8]radialene), 3482 (2) $[M]^-$ ([7]radialene), 2989 (8) $[M]^-$ ([6]radialene), 2489 (31) $[M]^-$ ([5]radialene), 1992 (100) $[M]^-$ ([4]radialene), 1494 (76) $[M]^-$ ([3]radialene); elemental analysis calcd (%) for $(C_{38}H_{42})_n$ [(498.75)$_n$]: C 91.51, H 8.49; found: C 91.37, H 8.47.

5,10,15,20-Tetrakis{3-[3,5-di(*tert*-butyl)phenyl]-1-[(3,5-di(*tert*-butyl)phenyl)ethynyl]prop-2-ynylidene}cycloicosa-1,3,6,8,11,13,16,18-octayne (27b), **5,10,15,20,25,30-Hexakis{3-[3,5-di(*tert*-butyl)phenyl]-1-[(3,5-di(*tert*-butyl)phenyl)ethynyl]prop-2-ynylidene}cyclotriaconta-1,3,6,8,11,13,16,18,21,23,26,28-dodecayne (27d)**, and **5,10,15,20,25,30,35,40-Octakis{3-[3,5-di(*tert*-butyl)phenyl]-1-[(3,5-di(*tert*-butyl)phenyl)ethynyl]-prop-2-ynylidene}cyclotetraconta-1,3,6,8,11,13,16,18,21,23,26,28,31,33-tetradecayne (27f)**: A solution of **12** (61 mg, 0.046 mmol) in THF (25 mL) and H_2O (1.2 mL) was treated with a solution of Bu_4NF in THF (1M, 0.5 mL). After stirring overnight, Et_2O (200 mL) was added and the mixture was washed with H_2O (2 × 200 mL). The organic phase was dried ($MgSO_4$) and then concentrated in vacuo without heating. The residue was redissolved in CH_2Cl_2 (170 mL), and a solution of Hay catalyst (1.1 mL) was added. After stirring for 3.5 h, the solvent was removed in vacuo and the residue purified on a short column (silica gel; hexanes/CH_2Cl_2 3:1), affording a mixture of **27b**,**d**,**f**, together with some higher mass impurities (GPC). The mixture was separated by gravity GPC (CH_2Cl_2), providing **27b** (4 mg, 9%) as a red oily solid, **27d** (6 mg, 13%) as an orange solid, and **27f** (4 mg, 9%) as a red-orange oily solid. **27b**: Analytical GPC (THF, 40 °C, λ = 400 nm): t_R = 16.3 min; ^{1}H NMR (200 MHz, $CDCl_3$): δ = 7.35 (s, 24H), 1.17 (s, 144H); ^{13}C NMR (125 MHz): δ = 151.0, 126.4, 124.3, 121.1, 119.0, 113.9, 103.6, 86.6, 86.4, 84.2, 34.7, 31.1; IR (CCl_4): $\tilde{\nu}$ = 2965 (s), 2929 (m), 2905 (w), 2867 (w), 2180 (w), 1589 (w), 1477 (w), 1466 (w), 1449 (w), 1434 (w), 1394 (w), 1363 (w), 1260 (w), 1248 (w), 1152 (w), 1097 (w), 1069 (w), 879 (w); UV/Vis ($CHCl_3$): 285 (37400), 298 (37300), 314 (33200), 379 (*sh*, 32900), 399 (37500), 468 (83000), 505 (*sh*, 51100); MALDI-TOF-MS (THA/citrate): *m*/*z*: 1993 $[M]^+$; **27d**: analytical GPC (THF, 40 °C, λ = 400 nm): t_R = 15.8 min; m.p.: decomposing to a black solid at ca. 160 °C, which melts > 250 °C; ^{1}H NMR (200 MHz, $CDCl_3$): δ = 7.42 (d, J = 1.7 Hz, 24H), 7.36 (t, J = 1.7 Hz, 12H), 1.23 (s, 216H); ^{13}C NMR (125 MHz): δ = 151.0, 126.6, 124.3, 123.2, 121.1, 114.1, 104.1, 86.6, 83.2, 83.0, 34.7, 31.2; IR (CCl_4): $\tilde{\nu}$ = 2963 (s), 2927 (m), 2904 (w), 2864 (w), 2183 (m), 1588 (w), 1477 (w), 1465 (w), 1449 (w), 1435 (w), 1393 (w), 1363 (w), 1247 (w), 1156 (w), 1098 (w), 877 (w); UV/Vis ($CHCl_3$): 255 (101000), 294 (97300), 303 (*sh*, 92700), 376 (*sh*, 89100), 389 (104000), 424 (94900), 445 (97300), 499 (*sh*, 60200); MALDI-TOF-MS (CH_2Cl_2/THA/citrate): *m*/*z*: 2993 $[M]^+$, 5986 $[2M]^+$; X-ray: see Figure 3; **27f**: analytical GPC (THF, 40 °C, λ = 400 nm): t_R = 15.4 min; ^{1}H NMR (200 MHz, $CDCl_3$): δ = 7.42 (d, J = 1.8 Hz, 32H), 7.35 (t,

0947-6539/01/0715-3278 $ 17.50+.50/0 *Chem. Eur. J.* **2001**, *7*, No. 15

$J = 1.8$ Hz, 16H), 1.23 (s, 288H); ^{13}C NMR (125 MHz): $\delta = 151.1$, 126.6, 124.3, 123.7, 121.1, 113.9, 104.1, 86.6, 83.3, 82.8, 34.7, 31.2; IR (CCl_4): $\tilde{\nu} =$ 2963 (s), 2928 (m), 2901 (w), 2866 (w), 2181 (m), 1588 (w), 1476 (w), 1465 (w), 1448 (w), 1435 (w), 1394 (w), 1363 (w), 1260 (w), 1247 (w), 1114 (w), 878 (w); UV/Vis ($CHCl_3$): 263 (142000), 292 (139000), 304 (*sh*, 126000), 373 (*sh*, 125000), 388 (148000), 417 (135000), 445 (126000), 508 (*sh*, 84600); MALDI-TOF-MS (THA/citrate): m/z: 3990 $[M]^+$.

Acknowledgements

Dr. Carlo Thilgen (ETHZ) is gratefully acknowledged for help in the nomenclature of the compounds. We thank Dr. N. Tirelli (ETHZ) for the evaluation of mesogenic properties. This work was supported by the Swiss National Science Foundation and the ETH Research Council. Y.G.B. was supported by a postdoctoral fellowship from the Korean Foundation of Science and Engineering (KOSEF) and M.B.N. acknowledges the receipt of a travel grant from The Danish Natural Science Research Council (S.N.F.).

[1] a) G. W. Griffin, L. I. Peterson, *J. Am. Chem. Soc.* **1963**, *85*, 2268–2273; b) L. Trabert, H. Hopf, *Liebigs Ann. Chem.* **1980**, 1786–1800; c) G. Köbrich, H. Heinemann, *Angew. Chem.* **1965**, *77*, 594–595; d) H. Bock, G. Rohn, *Helv. Chim. Acta* **1991**, *74*, 1221–1232; e) P. A. Waitkus, E. B. Sanders, L. I. Peterson, G. W. Griffin, *J. Am. Chem. Soc.* **1967**, *89*, 6318–6327; f) E. Heilbronner, *Theor. Chim. Acta* **1966**, *4*, 64–68; g) P. A. Waitkus, L. I. Peterson, G. W. Griffin, *J. Am. Chem. Soc.* **1966**, *88*, 181–183; h) E. A. Dorko, *J. Am. Chem. Soc.* **1965**, *87*, 5518–5520; i) M. Iyoda, H. Otani, M. Oda, Y. Kai, Y. Baba, N. Kasai, *J. Chem. Soc. Chem. Commun.* **1986**, 1794–1796; j) M. Iyoda, S. Tanaka, H. Otani, M. Nose, M. Oda, *J. Am. Chem. Soc.* **1988**, *110*, 8494–8500; k) T. Lange, V. Gramlich, W. Amrein, F. Diederich, M. Gross, C. Boudon, J.-P. Gisselbrecht, *Angew. Chem.* **1995**, *107*, 898–901; *Angew. Chem. Int. Ed. Engl.* **1995**, *34*, 805–809.

[2] For a review on radialenes, see: H. Hopf, G. Maas, *Angew. Chem.* **1992**, *104*, 953–977; *Angew. Chem. Int. Ed. Engl.* **1992**, *31*, 931–954.

[3] a) B. Heinrich, A. Roedig, *Angew. Chem.* **1968**, *80*, 367–368; *Angew. Chem. Int. Ed. Engl.* **1968**, *7*, 375; b) L. Trabert, H. Hopf, *Liebigs Ann. Chem.* **1980**, 1786; c) F. P. van Remoortere, F. P. Boer, *J. Am. Chem. Soc.* **1970**, *92*, 3355–3360.

[4] a) T. Fukumaga, M. D. Gordon, P. J. Krusic, *J. Am. Chem. Soc.* **1976**, *98*, 611–613; b) T. A. Blinka, R. West, *Tetrahedron Lett.* **1983**, *24*, 1567–1568; c) G. Seitz, R. Sutrisno, B. Gerecht, G. Offerman, R. Schmidt, W. Massa, *Angew. Chem.* **1982**, *94*, 290–291; *Angew. Chem. Int. Ed. Engl.* **1982**, *21*, 283; d) G. Seitz, G. Offermann, *Synthesis* **1984**, 752–753.

[5] a) R. O. Uhler, H. Schechter, G. V. D. Tiers, *J. Am. Chem. Soc.* **1962**, *84*, 3397–3398; b) H. Bock, G. Rohn, *Helv. Chim. Acta* **1992**, *75*, 160–169; c) M. Iyoda, H. Otani, M. Oda, Y. Kai, Y. Baba, N. Kasai, *J. Am. Chem. Soc.* **1986**, *108*, 5371–5372; d) T. Sugimoto, Y. Misaki, T. Kajita, Z. Yoshida, Y. Kai, N. Kasai, *J. Am. Chem. Soc.* **1987**, *109*, 4106–4107; e) T. Sugimoto, Y. Misaki, T. Kajita, T. Nagatomi, Z. Yoshida, Y. Yamauchi, *Angew. Chem.* **1988**, *100*, 1129–1131; *Angew. Chem. Int. Ed. Engl.* **1988**, *27*, 1078–1080; f) M. Iyoda, H. Otani, M. Oda, *Angew. Chem.* **1988**, *100*, 1131–1132; *Angew. Chem. Int. Ed. Engl.* **1988**, *27*, 1080–1081; g) T. Sugimoto, Y. Misaki, Z. Yoshida, J. Yamauchi, *Mol. Cryst. Liq. Cryst.* **1989**, *176*, 259–270; h) K. Takahashi, M. Ogiyama, *Chem. Lett.* **1991**, 129–132; i) M. Iyoda, H. Kurata, M. Oda, C. Okubo, K. Nishimoto, *Angew. Chem.* **1993**, *105*, 97–99; *Angew. Chem. Int. Ed. Engl.* **1993**, *32*, 89–90; j) K. Komatsu, H. Kamo, R. Tsuji, K. Takeuchi, *J. Org. Chem.* **1993**, *58*, 3219–3221; k) K. Kano, T. Sugimoto, Y. Misaki, T. Enoki, H. Hatakeyama, H. Oka, Y. Hosotani, Z. Yoshida, *J. Phys. Chem.* **1994**, *98*, 252–258; l) H. Uno, K. Kasahara, N. Nibu, S. Nagaoka, N. Ono, *J. Org. Chem.* **2000**, *65*, 1615–1622.

[6] a) A. M. Boldi, F. Diederich, *Angew. Chem.* **1994**, *106*, 482–485; *Angew. Chem. Int. Ed. Engl.* **1994**, *33*, 468–471; b) J. Anthony, A. M. Boldi, C. Boudon, J.-P. Gisselbrecht, M. Gross, P. Seiler, C. B. Knobler, F. Diederich, *Helv. Chim. Acta* **1995**, *78*, 797–817.

[7] For reviews on acetylenic molecular scaffolding, see: a) F. Diederich, *Nature* **1994**, *369*, 199–207; b) L. T. Scott, M. J. Cooney, in *Modern Acetylene Chemistry* (Eds.: P. J. Stang, F. Diederich), VCH, **1995**, pp. 321–351; c) U. H. F. Bunz, Y. Rubin, Y. Tobe, *Chem. Soc. Rev.* **1999**, *28*, 107–119; d) U. H. F. Bunz, *Top. Curr. Chem.* **1999**, *201*, 131–161; e) F. Diederich, L. Gobbi, *Top. Curr. Chem.* **1999**, *201*, 43–79; f) F. Diederich, *Chem. Commun.* **2001**, 219–227.

[8] A strategy for preparing expanded radialenes of the oligo-monoacetylene family ($C_{2n}H_n$), as well as hybrid expanded radialenes, has recently been developed: a) S. Eisler, R. R. Tykwinski, *Angew. Chem.* **1999**, *111*, 2138–2141; *Angew. Chem. Int. Ed.* **1999**, *38*, 1940–1943; b) R. R. Tykwinski, *Chem. Commun.* **1999**, 905–906.

[9] a) Ch. Bosshard, R. Spreiter, P. Günter, R. R. Tykwinski, M. Schreiber, F. Diederich, *Adv. Mater.* **1996**, *8*, 231–234; b) R. R. Tykwinski, M. Schreiber, V. Gramlich, P. Seiler, F. Diederich, *Adv. Mater.* **1996**, *8*, 226–231; c) R. Spreiter, Ch. Bosshard, G. Knöpfle, P. Günter, R. R. Tykwinski, M. Schreiber, F. Diederich, *J. Phys. Chem. B* **1998**, *102*, 29–32; d) R. R. Tykwinski, U. Gubler, R. E. Martin, F. Diederich, Ch. Bosshard, P. Günter, *J. Phys. Chem. B* **1998**, *102*, 4451–4465; e) Ch. Bosshard, in *Nonlinear Optical Effects and Materials* (Ed.: P. Günter), Springer Verlag, **2000**, pp. 7–161.

[10] a) J. Anthony, A. M. Boldi, Y. Rubin, M. Hobi, V. Gramlich, C. B. Knobler, P. Seiler, F. Diederich, *Helv. Chim. Acta* **1995**, *78*, 13–45; b) R. R. Tykwinski, M. Schreiber, R. P. Carlón, F. Diederich, V. Gramlich, *Helv. Chim. Acta* **1996**, *79*, 2249–2281; c) T. Lange, J.-D. van Loon, R. R. Tykwinski, M. Schreiber, F. Diederich, *Synthesis* **1996**, 537–550; d) R. R. Tykwinski, F. Diederich, *Liebigs Ann./Recueil* **1997**, 649–661.

[11] For a recent review on acetylenic coupling, see: P. Siemsen, R. C. Livingston, F. Diederich, *Angew. Chem.* **2000**, *112*, 2740–2767; *Angew. Chem. Int. Ed.* **2000**, *39*, 2632–2657.

[12] For a preliminary communication of parts of this work, see: M. Schreiber, R. R. Tykwinski, F. Diederich, R. Spreiter, U. Gubler, Ch. Bosshard, I. Poberaj, P. Günter, C. Boudon, J.-P. Gisselbrecht, M. Gross, U. Jonas, H. Ringsdorf, *Adv. Mater.* **1997**, *9*, 339–343.

[13] K. Sonogashira in *Metal-catalyzed Cross-coupling Reactions* (Eds.: F. Diederich, P. J. Stang), Wiley-VCH, **1998**, pp. 203–229.

[14] A. S. Hay, *J. Org. Chem.* **1962**, *27*, 3320–3321.

[15] a) A. M. Boldi, J. Anthony, C. B. Knobler, F. Diederich, *Angew. Chem.* **1992**, *104*, 1270–1271; *Angew. Chem. Int. Ed. Engl.* **1992**, *31*, 1240–1242; b) A. M. Boldi, J. Anthony, V. Gramlich, C. B. Knobler, C. Boudon, J.-P. Gisselbrecht, M. Gross, F. Diederich, *Helv. Chim. Acta* **1995**, *78*, 779–796.

[16] D. Philp, V. Gramlich, P. Seiler, F. Diederich, *J. Chem. Soc. Perkin Trans. 2* **1995**, 875–886.

[17] R. Faust, F. Diederich, V. Gramlich, P. Seiler, *Chem. Eur. J.* **1995**, *1*, 111–117.

[18] For the use of this mesogenic group in conjugated π systems, see: C. Thobie-Gautier, Y. Bouligand, A. Gorgues, M. Jubault, J. Roncali, *Adv. Mater.* **1994**, *6*, 138–142.

[19] a) A. C. Griffin, S. R. Vaidya, *Mol. Cryst. Liq. Cryst.* **1989**, *173*, 85–88; b) Z. Komiya, R. R. Schrock, *Macromolecules* **1993**, *26*, 1393–1401; c) A. W. Hall, D. Lacey, J. S. Hill, D. G. McDonnell, *Supramol. Sci.* **1994**, *1*, 21; d) M. Ungerank, B. Winkler, E. Eder, F. Stelzer, *Macromol. Chem. Phys.* **1995**, *196*, 3623–3641.

[20] G. Eglinton, A. R. Galbraith, *Chem. Ind.* (*London*) **1956**, 737–738.

[21] For the estimation of molecular weights (M_W) from GPC retention times (t_R), based on a polystyrene calibration curve, we employed the linear fit: $\log(M_W) = -0.2559059\,t_R + 7.534795$.

[22] The carbon resonances were assigned on the basis of relative intensities and by comparison to simpler derivatives.

[23] a) A. Krebs, J. Wilke, *Top. Curr. Chem.* **1983**, *109*, 189–233; b) R. Gleiter, D. Kratz, W. Schäfer, V. Schehlmann, *J. Am. Chem. Soc.* **1991**, *113*, 9258–9264; c) S. Eisler, R. McDonald, G. R. Loppnow, R. R. Tykwinski, *J. Am. Chem. Soc.* **2000**, *122*, 6917–6928.

[24] M. J. Edelmann, M. A. Estermann, V. Gramlich, F. Diederich, *Helv. Chim. Acta* **2001**, *84*, 473–480.

[25] For a discussion of the calculated and measured low barriers to rotation about C(sp)–C(sp^2) single bonds in 1,2-diphenylacetylene (tolane), see: a) J. K. Young, J. S. Moore in *Modern Acetylene Chemistry* (Eds.: P. J. Stang, F. Diederich), VCH, Weinheim, **1995**, pp. 415–442; b) J. M. Seminario, A. G. Zacarias, J. M. Tour, *J. Am. Chem. Soc.* **1999**, *121*, 411–416.

[26] R. Kahn, R. Fourme, D. André, M. Renaud, *Acta Crystallogr. Sect. B* **1973**, *29*, 131–138.

[27] a) A. de Meijere, S. Kozhushkov, T. Haumann, R. Boese, C. Puls, M. J. Cooney, L. T. Scott, *Chem. Eur. J.* **1995**, *1*, 124 – 131; b) M. Brake, V. Enkelmann, U. H. F. Bunz, *J. Org. Chem.* **1996**, *61*, 1190 – 1191.
[28] For a recent discussion on steric overcrowding in [*n*]radialenes, see: M. Kaftory, M. Botoshansky, S. Hyoda, T. Watanabe, F. Toda, *J. Org. Chem.* **1999**, *64*, 2287 – 2292.
[29] a) W. Marsh, J. D. Dunitz, *Helv. Chim. Acta* **1975**, *58*, 707 – 712; b) G. Wilke, *Angew. Chem.* **1988**, *100*, 189 – 211; *Angew. Chem. Int. Ed. Engl.* **1988**, *27*, 185 – 206.
[30] a) H. A. Staab, K. Neunhoeffer, *Synthesis* **1974**, 424; b) D. Venkataraman, S. Lee, J. Zhang, J. S. Moore, *Nature* **1994**, *371*, 591 – 593; c) O. Y. Mindyuk, M. R. Stetzer, P. A. Heiney, J. C. Nelson, J. S. Moore, *Adv. Mater.* **1998**, *10*, 1363 – 1366; d) P.-H. Ge, W. Fu, W. A. Herrmann, E. Herdtweck, C. Campana, R. D. Adams, U. H. F. Bunz, *Angew. Chem.* **2000**, *112*, 3753 – 3756; *Angew. Chem. Int. Ed.* **2000**, *39*, 3607 – 3610.
[31] S. Höger, V. Enkelmann, K. Bonrad, C. Tschierske, *Angew. Chem.* **2000**, *112*, 2356 – 2358; *Angew. Chem. Int. Ed.* **2000**, *39*, 2268 – 2270.
[32] For experimental and computational investigations on the electron-accepting properties of TEE derivatives, see: a) J. Anthony, C. Boudon, F. Diederich, J. P. Gisselbrecht, V. Gramlich, M. Gross, M. Hobi, P. Seiler, *Angew. Chem.* **1994**, *106*, 794 – 798; *Angew. Chem. Int. Ed. Engl.* **1994**, *33*, 763 – 766; b) ref. [22b]; c) C. Boudon, J. P. Gisselbrecht, M. Gross, J. Anthony, A. M. Boldi, R. Faust, T. Lange, D. Philp, J.-D. van Loon, F. Diederich, *J. Electroanal. Chem.* **1995**, *394*, 187 – 197; d) A. Hilger, J. P. Gisselbrecht, R. R. Tykwinski, C. Boudon, M. Schreiber, R. E. Martin, H. P. Lüthi, M. Gross, F. Diederich, *J. Am. Chem. Soc.* **1997**, *119*, 2069 – 2078; e) L. Gobbi, N. Elmaci, H. P. Lüthi, F. Diederich, *ChemPhysChem* **2001**, *2*, in press.
[33] For other investigations on cross-conjugation effects in extended macrocyclic and acyclic π-systems, see: a) Y. Zhao, R. R. Tykwinski, *J. Am. Chem. Soc.* **1999**, *121*, 458 – 459; b) Y. Zhao, R. McDonald, R. R. Tykwinski, *Chem. Commun.* **2000**, 77 – 78; c) S. C. Ciulei, R. R. Tykwinski, *Org. Lett.* **2000**, *2*, 3607 – 3610.
[34] a) Z. R. Grabowski, K. Rotkiewicz, A. Siemiarczuk, D. J. Cowley, W. Baumann, *Nouv. J. Chem.* **1979**, *3*, 443 – 454; b) K. Rotkiewicz, K. H. Grellmann, Z. R. Grabowski, *Chem. Phys. Lett.* **1973**, *19*, 315 – 318; c) K. Rotkiewicz, Z. R. Grabowski, A. Kowczynski, W. Kühnle, *J. Luminescence* **1976**, *12/13*, 877 – 885.
[35] a) W. Rettig, *Top. Curr. Chem.* **1994**, *169*, 253 – 299; b) W. Rettig, *Angew. Chem.* **1986**, *98*, 969 – 986; *Angew. Chem. Int. Ed. Engl.* **1986**, *25*, 971 – 988; c) W. Rettig, B. Bliss, K. Dirnberger, *Chem. Phys. Lett.* **1999**, *305*, 8 – 14.
[36] A. Hilger, J.-P. Gisselbrecht, R. R. Tykwinski, C. Boudon, M. Schreiber, R. E. Martin, H. P. Lüthi, M. Gross, F. Diederich, *J. Am. Chem. Soc.* **1997**, *119*, 2069 – 2078.
[37] R. E. Martin, U. Gubler, C. Boudon, Ch. Bosshard, J.-P. Gisselbrecht, P. Günter, M. Gross, F. Diederich, *Chem. Eur. J.* **2000**, *6*, 4400 – 4412.
[38] M. Ruben, E. Breuning, J.-P. Gisselbrecht, J.-M. Lehn, *Angew. Chem.* **2000**, *112*, 4312 – 4315; *Angew. Chem. Int. Ed.* **2000**, *39*, 4139 – 4142.
[39] J. Zyss, *Molecular Nonlinear Optics*: *Materials*, *Physics and Devices*, Academic Press, Boston, **1993**.
[40] a) Ch. Bosshard, U. Gubler, P. Kaatz, W. Mazerant, U. Meier, *Phys. Rev. B* **2000**, *61*, 10688 – 10701; b) U. Gubler, Ch. Bosshard, *Phys. Rev. B* **2000**, *61*, 10702 – 10710.
[41] F. Kajzar, J. Messier, *Phys. Rev. A* **1985**, *32*, 2352 – 2363.
[42] SHELXTL PLUS, Siemens Analytical X-ray Instruments Inc., Madison, USA, **1990**.
[43] A. Altomare, G. Cascarano, C. Giacovazzo, A. Guagliardi, M. Burla, G. Polidori, M. Camalli, *J. Appl. Crystallogr.* **1994**, *27*, 435.
[44] G. M. Sheldrick, SHELXL-97, *Program for the Refinement of Crystal Structures*, University of Göttingen, Germany, **1997**.

Received: January 31, 2001 [F3042]

  0947-6539/01/0715-3280 $ 17.50+.50/0